UNCLASSIFIED

AD NUMBER

AD-358 121

CLASSIFICATION CHANGES

TO   **UNCLASSIFIED**

FROM   **CONFIDENTIAL**

AUTHORITY

DNA via Ltr; Nov 30, 1980

THIS PAGE IS UNCLASSIFIED

AD NUMBER

AD-358 121

NEW LIMITATION CHANGE

TO

DISTRIBUTION STATEMENT: A

Approved for public release; Distribution is unlimited.

LIMITATION CODE: 1

FROM   No Prior DoD Distr Scty Cntrl St'mt Assgn'd

AUTHORITY

DNA via Ltr; Nov 30, 1980

OPERATION
PLUMBBO
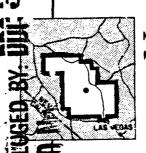
NEVADA TEST SITE
MAY–OCTOBER 1957

Project 6.1

MINE-FIELD CLEARANCE by NUCLEAR WEAPONS (U)

Issuance Date: August 16, 1960

HEADQUARTERS FIELD COMMAND
DEFENSE ATOMIC SUPPORT AGENCY
SANDIA BASE, ALBUQUERQUE, NEW MEXICO

CATALOGED BY: DDC 558121
AS AN

35 8121 L

19990514095

435
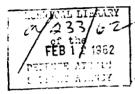
icument consists of 112 pages.

of 210 copies, Series A

OB

LEAR

Inquiries relative to this report may be mad

Chief, Defense Atomic Support Agency
Washington 25, D. C.

When no longer required, this document may
destroyed in accordance with applicable secu
regul.tions.

DO NOT RETURN THIS DOCUMENT

ABC Tec

UNCLASSIFIED

AD *358121*

UNCLASSIFIED

WT—1435

OPERATION PLUMBBOB—PROJECT 6.1

MINE-FIELD CLEARANCE by

F. E
Feli
Rob

Mid
Kan

U.S.
De
Forl

1ade to

y

nay be
ecurity

WT-1435

OPERATION PLUMBBOB—PROJECT 6.1

MINE-FIELD CLEARANCE by NUCLEAR WEAPONS (U)

F. E. Deeds, Capt. USA
Felix W. Fleming
Robert K. Stump

Midwest Research Institute
Kansas City, Missouri

U.S. Army Engineer Research and
  Development Laboratories
Fort Belvoir, Virginia

3

DDC CONTROL
NO. 51075

FOREWORD

This report presents the final results of one of the 46 projects comprising the military-effect program of Operation Plumbbob, which included 24 test detonations at the Nevada Test Site in 1957.

For overall Plumbbob military-effects information, the reader is referred to the "Summary Report of the Director, DOD Test Group (Programs 1–9)," ITR–1445, which includes: (1) a description of each detonation, including yield, zero-point location and environment, type of device, ambient atmospheric conditions, etc.; (2) a discussion of project results; (3) a summary of the objectives and results of each project; and (4) a listing of project reports for the military-effect program.

ABSTRACT

The objective of the project was to investigate the behavior of pressure-activated antitank mines under air-blast loading from a nuclear detonation. Of particular interest were the reliability of current methods for predicting probability of land-mine actuation from nuclear detonations, the effect of burial depth on mine actuation, and the effect of sympathetic actuation in extending the range of mine clearance. In addition, a study was initiated to determine if special methods were needed for prediction of mine actuation at particular ranges of transition in the pressure-wave shape.

Fifteen mine types, both United States and foreign, were employed. Test results indicated: (1) the procedures for predicting mine actuation under nuclear detonations were reasonably accurate; (2) in the live mine fields, sympathetic actuation occurred among mines; (3) the response of the Universal Indicator Mines (UIM) increased with burial depths to a maximum value between 6 and 9 inches; and (4) the reliability of the actuation curves can be improved by laboratory testing of adequate sampling of mines.

Included within the project were four subprojects conducted by or for Picatinny Arsenal, Diamond Ordnance Fuze Laboratories (DOFL), Chemical Warfare Laboratory (CWL), and the United Kingdom.

The purpose of the study by Picatinny Arsenal was to evaluate the effectiveness of two experimental actuation devices, High Hat and Partner, in providing pressure-actuated mines with protection against blast effects of nuclear detonations. It was concluded that High Hat provided significantly improved resistance to clearance and warranted further development. Although Partner worked well at high overpressure, it was concluded that the value of the design was questionable at pressures less than 16 psi.

Chemical Warfare Laboratory attempted to determine qualitatively the ground contamination pattern produced by E-5 land mines detonated by a nuclear blast. Two mines were detonated by Shot Priscilla. Preliminary inspection showed that the contaminant was spread to a distance of 5 yards from the mine detonation. Analysis indicated a difference in the distribution of ground contamination patterns between mines detonated by the nuclear blast and those detonated individually prior to the test. Dust storms that followed the explosion may have been responsible for the observed difference.

A special program was instituted to test four British mines under conditions specified by British authorities. The objective was to supplement current British data on the behavior of these mines under nuclear-blast loading. A cursory examination was made after the blast to determine: (1) displacement of mine by blast, (2) damage to the mine body, and (3) functioning of the fuzes. Analysis will be performed by the British and the results determined are not a part of this test program nor are such results expected to be available.

5

PREFACE

CONTENTS

SECRET

8

SECRET

9

SECRET

SECRET

TABLES

SECRET

Chapter 1
INTRODUCTION

1.1 OBJECTIVE

The objective of this ·roject was to investigate the behavior of pressure-activated antitank mines under air-blast loading from a nuclear detonation. To represent the various actuation systems, mines from the United States and from NATO and other foreig. nations were used. The aspects of particular interest in the investigation were: (1) reliabil.ty of current methods for predicting the probability of land mine detonation from nuclear detonations, (2) effects of depth of burial upon the actuation of the mines, (3) effect of sympathetic actuation in extending the radius of clearance, and (4) percentage of mines actuated by the explosion. In addition, it was expected to determine if special methods for predicting mine actuation would be needed at particular ranges where transitions in the pressure wave shape occurred.

Picatinny Arsenal investigated the effectiveness of two experimental designs in providing pressure-actuated mines with protection against nuclear blast effects. The two designs were code-named High Hat and Partner.

Diamond Ordnance Fuze Laboratories (DOFL) investigated the vulnerability of three types of antitank influence mine fuzes subjected to nuclear detonation.

Chemical Warfare Laboratory (CWL) investigated the ground contamination pattern produced by E-5 chemical land mines which had been detonated by a nuclear detonation.

A special investigation was conducted for the United Kingdom to investigate the behavior of three types of British antitank mines and one British antipersonnel mine under blast loading from a nuclear weapon.

1.2 BACKGROUND

Minefield clearance projects were conducted in three previous operations at the NTS.

1.2.1 Operation Buster, Project 3.5, October 1951 (Reference 1).
Universal Indicator Mines (UIM) were employed at 0 and 6 inches of burial. It was found that readings from the UIM were greater at 6 inches of burial than at 0 inches of burial. This was in contradiction to high-explosive tests, where there was a reduction in UIM readings as the depth of burial increased. It was also found that scaling techniques for UIM readings developed for high-explosive tests were not adequate for atomic explosions and required modification. The radius of mine clearance was not as large as expected, due to an unexplained skip effect. It was also determined that weapons detonated at heights (in feet) greater than three times the cube root of the yield (in pounds) were not effective for minefield clearance.

1.2.2 Operation Snapper, Project 3.4, April 1952 (Reference 2).
The test was designed to study the unexplained phenomena of skip effect and the increase in mine actuation with burial depth found during the Buster test. The two effects were again observed. The shape of the initial portion of the pressure wave and the slow rise to peak pressure were proposed as possible answers to the skip phenomenon. The increase in mine actuation with depth of burial down to

SECRET

6 inches was thought to be caused by the shape of the incident pressure pulse and an extraneous surface effect. It was estimated that for optimum or near-optimum range of clearance, a weapon should be detonated at a height (in feet) equal to the cube root of the yield (in pounds).

1.2.3 Operation Upshot-Knothole, Project 3.18, March 1953 (Reference 3). Live mines were tested for the first time under a nuclear explosion. The M-15, M-6, M-14, and the UIM were employed. The skip effect and increase in actuation with depth of burial were again observed; however, the increase in pressure-plate deflection or mine actuation with depth was considered insignificant down to about 6 inches of burial, and beyond that depth deflection (or actuation) decreased. The first quantitative explanation that might account for part of the above phenomena was given. It was theoretically shown that if the pressure wave has a gradual rise to its maximum value, an increase in pressure-plate deflection can occur with an increase in burial depth. It was shown, also, that for the long pressure rise time, normal in nuclear blasts, static considerations should govern prediction of the activation of mines. The static response of mines to nuclear blasts is generally less than the mine response under dynamic high-explosive loading, the probable reason for the phenomenon formerly referred to as the skip effect. The live-minefield data showed that sympathetic actuation increased the range of mine clearance for M-6 mines. Sympathetic actuation or blast-induced actuation is the actuation of a mine caused by the explosion of another mine. In a nuclear detonation, the blast of a mine explosion may reinforce the basic pressure pulse and cause a greater percentage of actuation of adjacent mines.

1.3 WAVE THEORY AND LABORATORY ANALYSIS

To determine the effects of blast on pressure-activated mines, consideration has been given to both the variations of the shock pulse and the theory of mine actuation.

1.3.1 The Precursor Wave. The precursor wave phenomenon can have an important effect on the clearance of mines by blast. One of the essential differences between high-explosive and nuclear explosions is the tremendous thermal radiation associated with nuclear detonations. When the thermal radiation reaches the ground surface, a heated layer is formed at the earth's surface. This layer is composed of air and dust particles whose resultant density is considerably higher than the density of air. This layer is formed prior to the arrival of the shock at the ground-air interface. It is believed that this results in a higher particle velocity in this medium. Therefore, after reflection, a pressure wave (known as the precursor) travels along the ground ahead of the main shock. The succession of the two pulses results in a total pressure pulse of long duration with a long rise time to the peak pressure. Since some of the initial energy of the shock has been utilized in the creation of the precursor, the peak pressure is less than would have been expected from a free air shock at comparable ranges. The passage of this long-duration wave of slow rise time causes the mines to react as though undergoing static compression, rather than loading from a step impulse. This type of behavior is experienced until the main shock catches the precursor and the two merge into a single sharp shock front. In this latter region, the mines react as though struck by a suddenly applied load.

1.3.2 Laboratory Analysis and Mine-Actuation Theory. To evaluate mine behavior under blast-pressure loading, a contract was initiated by the Corps of Engineers with Midwest Research Institute. The objectives of this contract were to obtain extensive data on the characteristics of pressure-activated land mines under both static and dynamic loading and to develop a reliable theory to predict pressure-type mine actuation under varying conditions of loading, depth of burial, and type of soil (Reference 4). One of the simplest theories developed for mine actuation was to simulate the mine with a linear one-degree-of-freedom mass-spring system. In this analogy, the pressure plate was the mass, and the spring force of the pressure plate was the resisting force that was proportional to the displacement of the mass. In general, the loading force on the mine was suddenly applied; however, the theory was extended to give results with a gradually applied loading force. Procedures were developed for linearization of the actual

14

SECRET

non-linear pressure-plate spring force. The mine body was assumed rigid, and no consideration was given to soil elasticity under the mine. Consideration of the soil over the mine could be taken into account by the addition to the mass of the pressure-plate of a portion of the mass of the soil over the pressure-plate. The theory was developed primarily for long-duration (50 to 100 msec) pressure pulses of low amplitude (10 to 30 psi).

A comparison of the above theory with experimental data from a dynamic mine-loading device indicated that the theory predicted true mine-actuation pressures within 30 percent for a number of the mine types (TMi-43, UIM, M-15, TMDB, TM-41). This theory, in conjunction with the data on static mine characteristics, served as a basis for determining the overpressures at which the mines were to be placed.

Other, more-elaborate theories were developed to include the mass of the mine body, elasticity of the soil under the mine, and the behavior of the soil over the pressure plate. Detailed analysis of these theories is to be found in Reference 4.

SECRET

Chapter 2
PROCEDURE

2.1 SHOT PARTICIPATICN

The mine-field clearance test was conducted during Shot Priscilla in Frenchman Flat at the NTS. The device had a yield of 36.6 kt and was fired from a 700-foot balloon (1.67 times the cube root of the yield in pounds).

2.2 INSTRUMENTATION

A Ballistics Research Laboratories (BRL) self-recording pressure-time gage was placed in the center of each live mine field. Similar gages were placed at the beginning of the arc on the inert side of the mine field (Figure 2.1). It was anticipated that a comparison of any two records at the same ground distance would show the extent to which the pressure pulse from the detonation of live mines reinforced the basic nuclear pressure pulse. In addition, three special pressure-time gages, mounted in conventional M-15 mine cases, were buried with 9, 12, and 36 inches of cover at 1.250 feet from ground zero to test the gage performance and to supplement other pressure-time records.

Waterways Experiment Station (WES), under the auspices of Project 3.8, took random soil samples in Frenchman Flat of undisturbed soil and found good homogeneity down to depths of at least 4 feet. In addition, eleven samples of disturbed soil were taken at depths of from 3 to 36 inches. These samples were obtained from shafts which had been drilled and refilled, thereby simulating the actual procedure of mine burial. Each of the samples was analyzed to determine the density, water content, and modulus of deformation.

2.3 TEST ITEMS

The following mines were used in the test:

Origin	Type	Figure
USA	M-15	2.2
	M-19	2.3
	UIM	2.4
Danish	M/47-I	2.5
	M/47-II	2.6
	M/52	2.7
Italian	CC-48	2.8
	CS-42/3	2.9
	SACI	2.10
USSR	TMD-B	2.11
	TM-41	2.12
Belgian	PRB-ND-49	2.13
German	TMi-43	2.14
French	Model 1951	2.15
British	Mark VII	2.16

16

SECRET
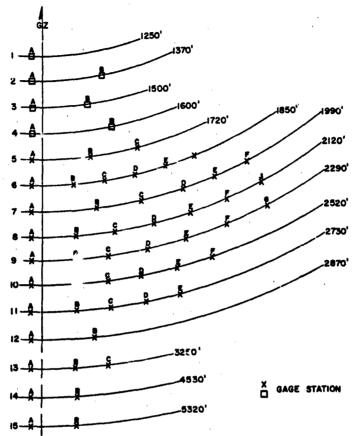
Figure 2.1 Layout of pressure-time gage stations.

Figure 2.2 USA, M-15.

17
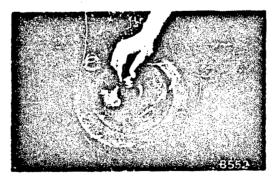
SECRET

Figure 2.4 USA, UIM.
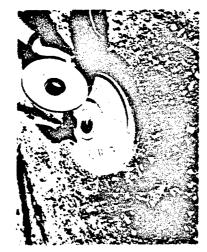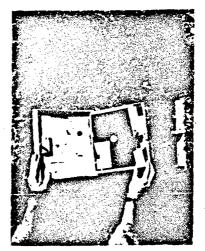
Figure 2.6 Danish, M/47-II.
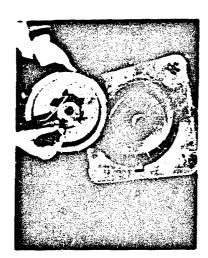
Figure 2.3 USA, M-19.
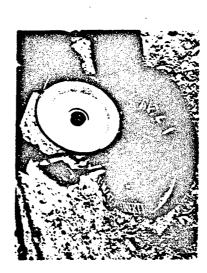
Figure 2.5 Danish, M/47-I.
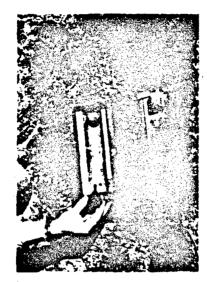
Figure 2.8 Italian, CC-48.

Figure 2.10 Italian, F .CI.

Figure 2.7 Danish, M/52.
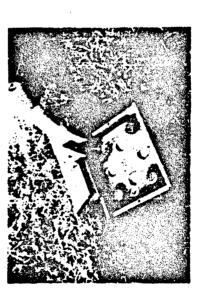
Figure 2.9 Italian, CS-42, .

19

SECRET
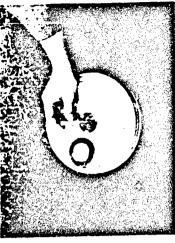
Figure 2.12 USSR, TM-41.

Figure 2.14 German, TMi-43.

Figure 2.11 USSR, TMD-B.
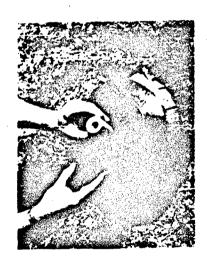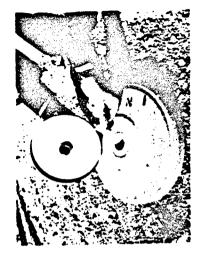
Figure 2.13 Belgium, PRB-ND-49.

SECRET

2.4 PLACEMENT

Estimated overpressures for the various probabilities of actuation are presented in Table 2.1.
Predicted overpressures as a function of range were taken from the official test predictions
(2.17). Probabilities of actuation were obtained from a statistical analysis of laboratory
(erence 4). Pressures for the location of mine fields to obtain 10, 50, and 90 percent
...ity of actuation were determined by combining this laboratory information with the pre-
dicted ranges. From the pretest predictions of the wave forms and the predicted pressures, it
appeared that the precursor would play a significant role in mine actuation to approximately
4,000 feet from ground zero. This meant that since the natural periods of the mines were short
compared to the predicted rise time of the atomic blast, static actuation pressures should be
used to determine the ranges at which most of the mines should be placed. The one exception
to this rule was the M-19 mine which was planted in fields determined by its response to dynamic
actuation pressures. Because limited information on actuation pressures for the M-19 was avail-
able, it was placed in fields in and on both sides of the estimated transition region (from a wave
of slow rise time to a sharp shock). These considerations, coupled with the availability of the
mines, led to the decision to place the M-19 in five fields covering a greater range of pressures.
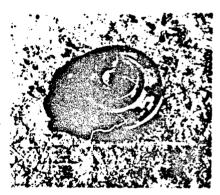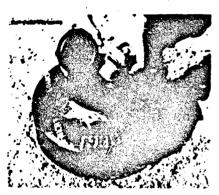
Figure 2.15 French, Model 1951.

Figure 2.16 British, Mark VII.

2.5 LAYOUT

The project layout is shown in Figure 2.18.

2.5.1 Inert and Live Mine Fields.
Mines in both the inert and live fields were buried with
$6 \pm \frac{3}{4}$ inches of soil cover. Placement holes were drilled by an earth auger with a 20-inch diam-
eter bit. The placement pattern for each type of mine in the inert mine fields is shown in Figure
2.19. Inert models of the M-52, PRB-ND-49 and M/47-II mines were equipped with live detona-
tors, since inert detonators were not available for these mines.

The live mine-field pattern is shown in Figure 2.20. Care was taken in the spacing of the
live mine fields (i.e., the spacing between each field) so that the effects of sympathetic detona-
tion, or actuation, would be confined within each field. The British Mark VII mine, which nor-
mally requires two pressure pulses for actuation, was mechanically armed when placed in a live
mine field so that a single pressure pulse could detonate the mine. This arming was necessary
since no recovery of live mines not detonated by the nuclear blast was to be made and therefore
it would not be possible to determine if the fuze had received sufficient pressure to arm the mine
if actuation did not occur.

2.5.2 Depth of Burial in Mine Fields.
Depth of burial is defined as the amount of cover over
the pressure plate of the mine. The UIM and TMi-43 mines were used in the depth-of-burial

21

TABLE 2.1 PLACEMENT PRESSURE LEVELS FOR MINES

All pressures in psi.

Country	Type of Mine	Predicted Pressure Level for Activation †										Selected Field Test, Pressure Levels †		
		1 Percent		10 Percent		50 Percent		90 Percent		99 Percent		10 Percent	50 Percent	90 Percent
		Static	Dynamic	Static	Dynamic	Static	Dynamic	Static	Dynamic	Static	Dynamic	Percent	Percent	Percent
USA	M-15	7.6	8.1	8.4	8.9	9.4	9.7	10.3	10.4	11.6	11.2	8	10	12
	M-19	—	6.3	—	6.8	—	7.5	—	8.2	—	8.8	6	8*	10
Belgium	PRB-ND-40	9.0	6.2	11.9	7.0	15.8	7.8	16.3	8.7	24.2	9.4	12	15	18
French	1951	12.5	6.3	28.3	14.2	42.6	21.3	56.7	28.4	72.6	38.3	25	40	50
British	Mark VII	16.8	14.1	21.0	15.8	23.2	17.4	25.4	18.0	27.8	20.7	20	25	30
Danish	M/47-I	15.9	11.3	18.8	13.2	21.7	15.2	24.4	17.1	27.3	19.1	18	21	25
	M/47-II	8.5	6.8	10.1	7.1	11.5	8.1	12.9	9.1	14.5	10.2	10	12	15
	M/53	8.0	7.0	10.4	9.3	11.9	10.6	13.4	11.9	15.0	13.3	10	12	15
German	TMi-43	39.2	18.4	42.6	20.0	46.8	21.6	49.1	23.1	52.4	24.6	40	50	60
USSR	TM-41	12.9	11.4	16.0	14.1	16.9	16.7	21.6	19.1	24.8	21.7	15	18	21
	TMD-B	11.9	7.8	15.1	8.9	18.0	11.8	21.2	13.9	24.4	16.0	15	18	21
Italian	CC-48	13.6	11.7	15.7	13.6	18.0	15.6	20.2	17.6	22.6	19.6	12	18	25
	CS-42.3	18.1	15.3	21.3	18.0	24.3	20.5	27.3	23.1	30.6	25.7	14	25	35
	SACI	15.5	8.4	18.2	9.9	20.8	11.3	23.4	12.7	26.1	14.2	15	21	30

* Fields were also placed at 6.5 and 9 psi.
† Probabilities of mine activation.

Figure 2.17 Predicted overpressures versus range.

23

SECRET
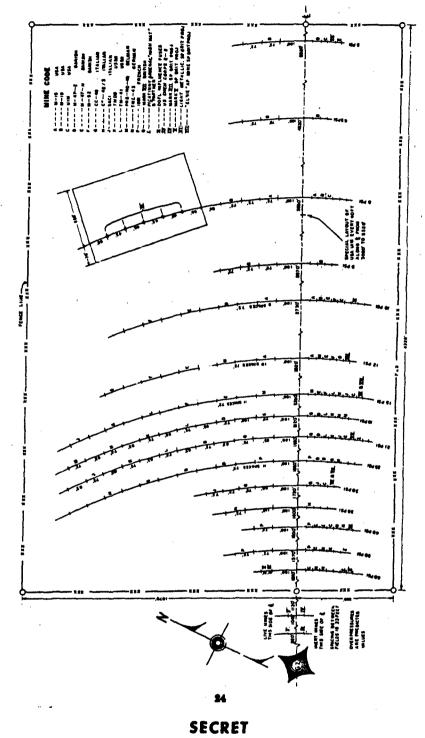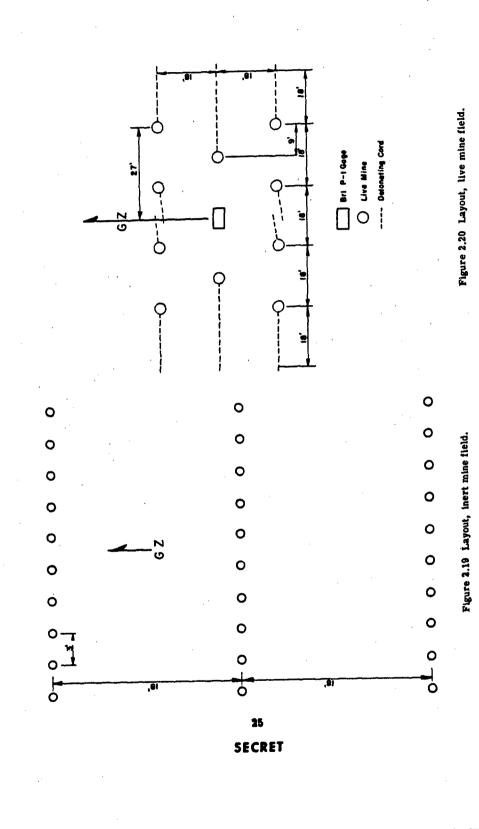
Figure 2.18 Project layout.

Bri P-1 Gage

Live Mine

Detonating Cord

Figure 2.20 Layout, live mine field.

27'

GZ

18'

18'

18'

9'

18'

18'

18'

18'

GZ

Figure 2.19 Layout, inert mine field.

18'

18'

25

investigation. The static pressure required to activate the TMi-43 mine ranged from 39.2 psi for 1-percent detonation to 52.4 psi for 99-percent detonation. Previous work indicated that there was good correlation between UIM readings and predictions of TMi-43 mine activation. Layout of a typical depth of burial field is shown in Figure 2.21. The UIM fields were placed at

DEPTH OF COVER
OVER MINES (IN.)
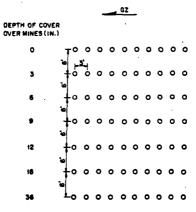
Figure 2.21 Layout, depth of burial.

ranges where overpressures of 5, 8, 10, 15, 21, 30, 40, 50, and 60 psi were predicted; two fields each of TMi-43 mines were placed at 40, 50, and 60 psi ranges. A complete description of the operation of the UIM is included in previous test reports (References 1, 2, and 3). Laboratory analysis by Midwest Research Institute indicated that the gap between the bottom of the pressure plate and the top of the fuze was a vital factor in determining the force for actuation. This information, coupled with the fact that the indicator readings in the region of 0 to 10 mils were of questionable reliability, led to a decision to increase the accuracy of measuring the response of the UIM in the lower pressure regions. Accuracy was increased by the setting of the indicator pin to within 2 mils from the under side of the pressure plate. Under these conditions, the deflection of the pressure plate could be measured when the deflection was less than 60 mils. The setting was not made at ranges and depths where it was believed that the deflection would exceed 60 mils.

For the same reasons, the gaps were also measured for all TMi-43 mines before placement.

2.5.3 Change from a Static to a Dynamic Pressure Pulse. In order to better determine the region where the main shock overtakes the precursor and the steep-fronted shock begins — (that is, where loading changes from static to dynamic), five UIM's were placed every 40 feet from 3,000 to 5,320 feet from ground zero all with 6 inches of earth cover (Figure 2.18). It was expected that the range of placement would provide indicator readings over this transition region. The ranges of 3,240 and 3,280 feet were omitted since there was already a UIM field at 3,250 feet from ground zero. On all these mines, the gap was set at 2 mils.

2.6 MINE-FIELD CLEARANCE PROCEDURES

Before each live mine was planted, a ½-pound charge of TNT, wrapped with detonating cord, was placed in the bottom of the hole. The detonating cord was placed in a 6-inch trench as shown in Figure 2.20. This provided a means of detonating any live mines that had not been actuated by the nuclear blast. Aerial photographs were taken of the entire mine-field area just prior to and just after the nuclear explosion. The pretest photograph was to be used for comparison with postshot photographs and for postshot recovery orientation. Oil drums filled with soil were placed at the corners of the fields for fiducial markers.

26

Chapter 3
RESULTS and DISCUSSION

The mine test results were satisfactory. Useful actuation data were obtained for most of the live and inert mines. The UIM and TMi-43 mines gave pertinent data concerning variation of mine behavior with depth of burial.

3.1 INSTRUMENTATION

3.1.1 Air-Blast Measurements. Of the 56 pressure-time records desired, only 28 complete records were obtained. Nineteen records presented only peak overpressure; six records were only partially complete; no records were obtained at three stations. Of the peak-pressure records, three were from peak-pressure gages. Pre-activation and gage malfunction, the causes of which are discussed in References 7 and 8, were factors which contributed to the loss of records.

For the special pressure-time gages mounted in M-15 mine cases placed at a range of 1,250 feet (actual overpressure of 76 psi), two of the three records were destroyed when the mine casing was crushed. The third record (Figure 3.1) served as a source of information for the pressure on a mine at a burial depth of 36 inches. It is believed that had a filler been placed in the air pocket around the gage, crushing would not have occurred.

Pressure results are compiled in Table 3.1. The graph in Figure 3.2 shows the predicted and experimental curves of peak overpressure versus range. The experimental curve was based on the results obtained from the gages on the inert side of the mine field and data from other projects. Figure 3.3 shows pressure-time records taken from stations where complete pressure-time histories were recorded.

The amplitude scale of the pressure-time record can be estimated from the peak pressure tabulated in Table 3.1. The time scale is approximately 62.5 msec/in for gages at Stations 1A, 2A, and 3A, and approximately 200 msec/in at all other stations.

3.1.2 Soil Calibration. Results from the various soil tests are shown in Table 3.2. Reference 5 gives additional details on soil measurements.

3.2 INERT AND LIVE MINE FIELDS

Results from the live and inert fields, along with actual overpressures and probability levels of actuation, are presented in Table 3.3. The data on each field are contained in Appendix E. Figure 3.4 is a postshot aerial photograph of the mine field area. It shows the general condition of the entire field. The craters pictured on the photograph indicate the number of live-mine detonations. This information was useful in planning recovery procedures.

3.2.1 Determination of Cumulative Probability Distributions. Air blast records show that the precursor in the 1,370 to 3,250-foot range had a reasonably sharp rise with the time to peak varying between 3 and 24 msec. The one-degree-of-freedom theory with a gradually applied load (Reference 4) indicates that for these rise times, most of the mines should respond with a pressure plate deflection greater than the deflection for a static load of the same amplitude. In other words, the mine response to the precursor is between purely static and totally dynamic. As a result, the peak pressure of the precursor necessary for actuation would be less than the static actuation pressure. The records did indicate that the precursor was sometimes respon-

27

SECRET

Figure 3.1 Pressure record, mine pressure gage.

⊙ Minefield Data
— Predicted
— Actual

Peak Overpressure, psi

Range x 10³ Feet
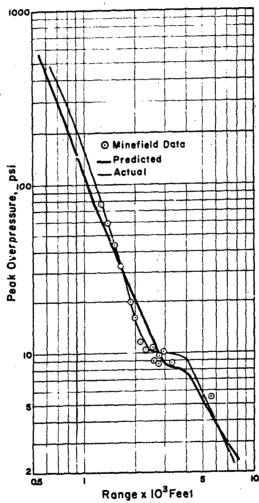
Figure 3.2 Overpressure versus ground range.

28

SECRET

STA 2A

STA 3A

STA 5A

STA 6A

STA 6D

STA 7A
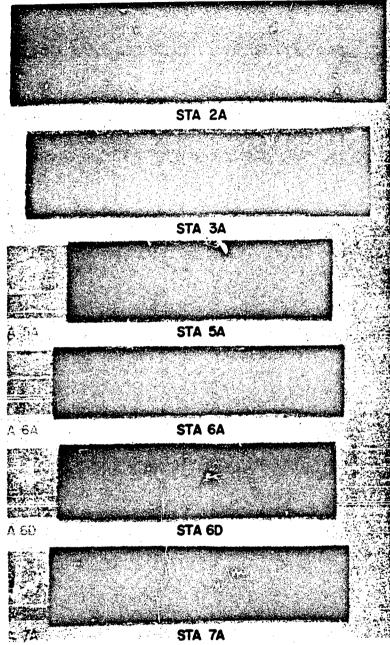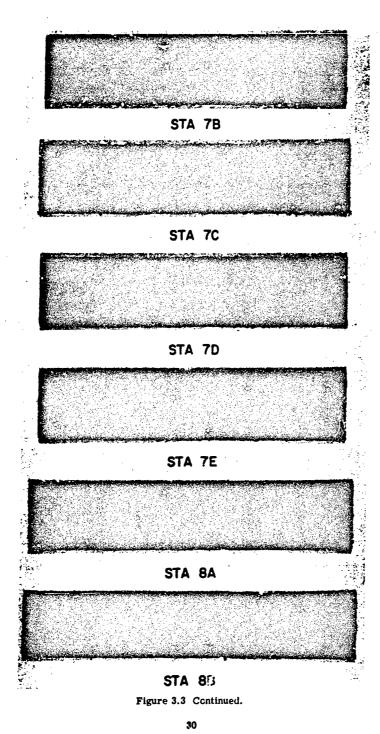
Figure 3.3 Pressure records.

29

STA 7B

STA 7C

STA 7D

STA 7E

STA 8A

STA 8B

Figure 3.3 Continued.

30

STA 8D

STA 8E

STA 8G

STA 9A

STA 9B

STA 9C

Figure 3.3 Continued.

31

STA 9C

STA 9E

STA 10A

STA 10D

STA 10F

Figure 3.3 Continued.

STA 11A

STA 11B

STA 11D

STA 13A

STA 13C

Figure 3.3 Continued.

1
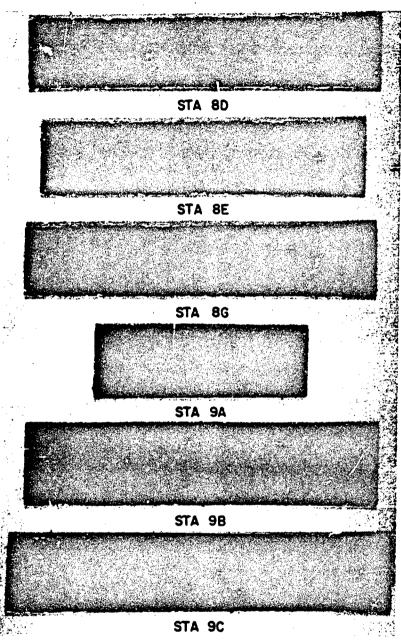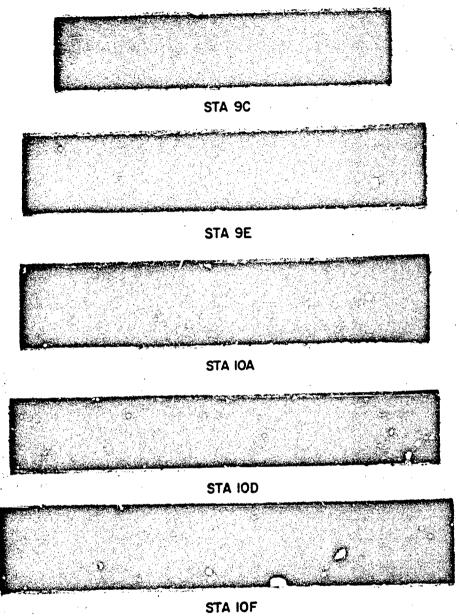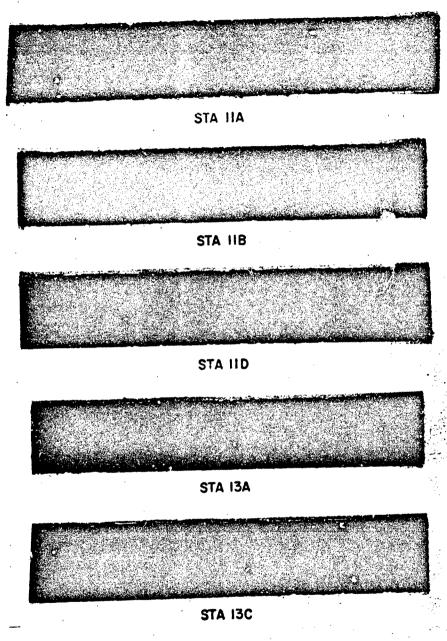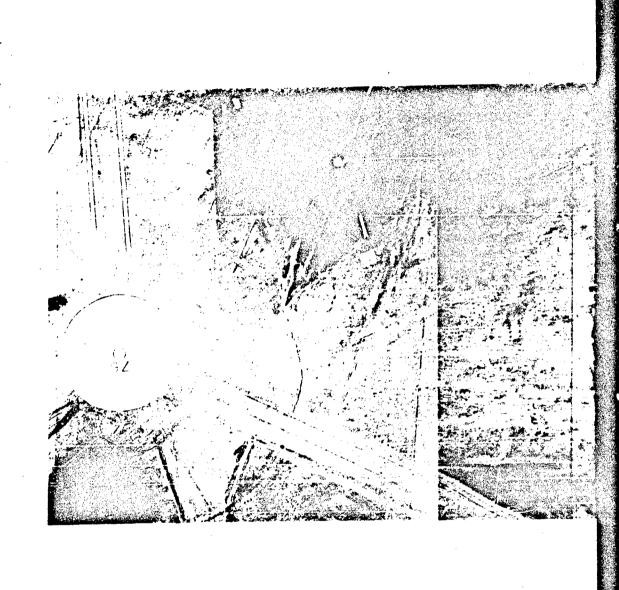
Figure 3.4 Postshot aerial photograph.

ph.

3
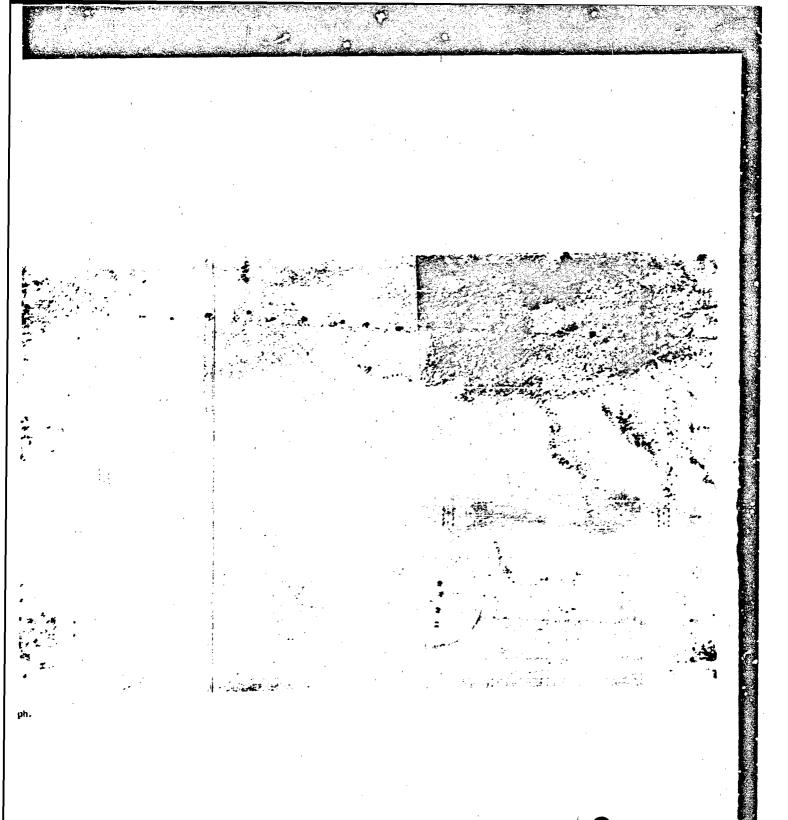
TABLE 3.1 AIR-BLAST MEASUREMENTS

Pressure Station	Range	Predicted Peak Overpressure	Recorded Peak Overpressure	Type of Live Minefield	Percent of Mines Activated	Remarks
	ft	psi	psi			
1A	1,250	60	76	None	—	Precursor incomplete
2A	1,370	50	60.5	None	—	
2B	—	—	53.7	1951	80	Peak pressure only
3A	1,500	40	43.6	None	—	
3B	—	—	43.0	1951	80	Peak pressure only
4A	1,600	35	33.3	None	—	Peak pressure only
4B	—	—	38.7	CS-42/3	90	Peak pressure only
5A	1,720	30	28.9	None	—	
5B	—	—	14.1	Mark VII	10	Main shock off scale
5C	—	—	14.4	SACI	30	Main shock off scale
6A	1,850	25	20.6	None	—	
6B	—	—	12.9	1951	40	Peak pressure only
6C	—	—	—	M/47-I	100	No record
6D	—	—	33.3	Mark VII	0	
6E	1,850	25	27.0	CC-48	40	Preactivated
6F	—	—	15.4	CS-42/3	70	Preactivated
7A	1,990	21	16.0	None	—	
7B	—	—	17.8	Mark VII	0	
7C	—	—	17.8	M/47-I	90	
7D	—	—	15.1	TM-41	10	
7E	—	—	16.2	TMD-B	10	
7F	—	—	36.9	SACI	10	Partial Record
8A	2,120	18	11.6	None	—	Preactivated
8B	—	—	13.7	CC-48	10	
8C	—	—	15.6	M/47-I	10	Preactivated
8D	—	—	13.9	TM-41	0	
8E	—	—	14.7	TMD-B	20	
8F	—	—	13.5	CS-42/3	20	Preactivated
8G	—	—	15.2	PRB-ND-49	100	
9A	2,290	15	10.4	None	—	
9B	—	—	12.6	PRB-ND-49	70	
9C	2,290	15	8.5	M/47-II	60	
9D	—	—	14.7	M/52	14.7	Preactivated
9E	—	—	10.5	TM-41	0	
9F	—	—	16.6	TMD-B	16.6	
9G	—	—	14.7	SACI	0	Preactivated
10A	2,520	12	10.9	None	—	
10B	—	—	11.1	M-15	0	Preactivated
10C	—	—	9.4	PRB-ND-49	0	Preactivated
10D	—	—	10.4	M/47-II	70	
10E	—	—	—	M/52	90	No Record
10F	—	—	9.9	CC-48	0	
11A	2,720	10	8.7	None	—	
11B	—	—	9.1	M-15	0	
11C	—	—	10.4	M-19	70	Preactivated
11D	—	—	10.7	M/47-II	60	
11E	—	—	9.2	M/52	10	
12A	2,870	9	10.0	None	—	Peak pressure gage used
12B	—	—	9.0	M-19	50	Peak pressure gage used
13A	3,250	8	8.7	None	—	
13B	—	—	9.7	M-15	0	Preactivated
13C	—	—	15.6	M-19	90	
14A	4,530	6.5	—	None	—	No record
14B	—	—	9.6	M-19	100	Peak pressure gage used
15A	5,330	5	5.4	None	—	Preactivated
15B	—	—	10.7	M-19	100	Motor did not run

37

SECRET

sible for actuating some of the mines. In the unusual soil conditions found in Frenchman Lake, where the precursor is pronounced, the maximum pressure may occur in the precursor and therefore corrections should be made to the predicted static actuation pressures to adjust for this dynamic effect.

Cumulative probability curves for each mine type were computed for static pressure loading by calculating an equivalent static pressure for the inert mine field data. On each curve the equivalent static points are plotted with the actual test points.

The procedure for fitting a cumulative probability distribution to the test points using normal probability theory is as follows:

$$P = P_a + y\sigma \tag{3.1}$$

Where: P = mine-field pressure
P_a = pressure for 50 percent mine actuation
σ = standard deviation of pressure
y = probability factor

The value of y is a function of the percentage of mines that actuated and is obtained from normal

TABLE 3.2 SOIL CALIBRATION

Measurement	Range	Average
Density	66.5 to 74.5 pcf	69.1 pcf
Water Content	4.9 to 12.0 pct	8.2 pct
Modulus of Deformation at 50 psi (disturbed soil)	685 to 927 psi	810 psi
Modulus of Deformation at 100 psi (disturbed soil)	1,400 to 2,080 psi	1,755 psi

probability tables. Values of y for various mine actuation percentages are tabulated in Table 3.4. The principle of least squares was applied to the data to obtain a straight-line fit.

$$P_a = \frac{\Sigma y^2 \Sigma P - \Sigma v \Sigma Py}{n \Sigma y^2 - (\Sigma y)^2} \tag{3.2}$$

$$\sigma = \frac{n\Sigma Py - \Sigma P \Sigma y}{n \Sigma y^2 - (\Sigma y)^2} \tag{3.3}$$

Where: n = number of mines in the field.

Once the above two parameters have been determined, the cumulative probability distribution can be plotted with the help of Table 3.4 and Equation 3.1. Because of the small sample size and the questionable reliability of certain pressure measurements, the percentages of mine actuation observed for the test must not be interpreted as the true values.

US M-19. The cumulative probability distribution of the M-19 mine is shown in Figure 3.5. Only three of the four test points were considered in determining the curve. The highest test point at 93.3 percent actuation was assumed to be in error and therefore discarded.

For the 93.3 percent actuation point, the true actuation percentage will lie between 72.1 and 99.2 percent in 99 cases out of 100. For the 46.7 percent actuation test point, the true percentage will fall between 24.0 and 70.6 percent. The lower limit of the 93.3 percent point does not overlap the upper limit of the 46.7 percent test point. For the true value to fall within the expectation limits of both simultaneously, there must be an overlap of limits, and the probability of this simultaneous occurrence is the product of the two levels considered. For the two points in question, a higher percentage level would have to be selected to obtain overlap. Since the expectation limits of the two points at the 99 percent probability level do not overlap, the wide difference be-

SECRET

TABLE 3.3 LIVE AND INERT MINE TEST RESULTS

Mine Type	Range	Peak Overpressure	Percent Actuated Actual	
			Live	Inert
	ft	psi *		
French 51	1,370	60.5	80	70.0
	1,500	43.6	80	60.0
	1,850	20.6	40	0
CS-42/3	1,600	33.3	90	96.7
	1,850	20.6	70	80.0
	2,120	11.6	20	60.0
Mark VII	1,720	28.9	30	3.3
	1,850	20.6	0	3.3
	1,990	16.0	0	0
SACI	1,720	28.9	30	6.7
	1,990	16.0	10	6.7
	2,290	10.4	0	3.3
M/47-I	1,850	20.6	100	50.0
	1,990	16.0	90	16.7
	2,120	11.6	10	26.7
TMD-B	1,990	16.0	10	20.0
	2,120	11.6	20	46.7
	2,290	10.4	10	43.3
TM-41	1,990	16.0	10	70.0
	2,120	11.6	0	86.7
	2,290	10.4	0	63.3
CC-48	1,850	20.0	40	46.7
	2,120	11.6	10	10.0
	2,520	10.9	0	13.3
PRB-ND-49	2,120	11.6	100	83.3
	2,290	10.4	70	76.7
	2,520	10.9	0	80.0
M/52	2,290	10.4	90	90.0
	2,520	10.9	90	90.0
	2,730	8.7	10	83.3
M/47-II	2,290	10.4	80	46.7
	2,520	10.9	70	66.7
	2,730	8.7	80	73.3
M-15	2,520	10.9	0	0
	2,730	8.7	0	0
	3,250	8.7	0	0
M-19	2,730	8.7	70	93.3
	2,870	10.0	50	63.3
	3,250	8.7	90	46.7
	4,530	†	100	100.1
	5,320	6.4	100	16.7

* Pressure values taken from gages placed on inert side of minefield.

† No record obtained.

TABLE 3.4 ABRIDGED CUMULATIVE NORMAL PROBABILITY DISTRIBUTION

Percent Mine Actuation	$y = \dfrac{P - P_A}{\sigma}$
0.5	−2.576
1.0	−2.326
2.5	−1.960
5.0	−1.645
10.0	−1.282
15.0	−1.036
20.0	−0.842
25.0	−0.674
30.0	−0.524
35.0	−0.385
40.0	−0.253
45.0	−0.126
50.0	0
55.0	0.126
60.0	0.253
65.0	0.385
70.0	0.524
75.0	0.674
80.0	0.842
85.0	1.036
90.0	1.282
95.0	1.645
97.5	1.960
99.0	2.326
99.5	2.576

tween these two points would occur less than 2 percent of the time in a random sample. If such an extreme sample were encountered, an error would result in its use. Discounting the possibility of such an extreme sample, then one or both of the points must be in error. In view of the relative position of the other test points, there is a greater likelihood of the upper point being in error than the lower point. Therefore the high point was discarded as either being in error or coming from an extreme sample.

US M-15. Test results of the M-15 mine (Table 3.3) show that none of the mines actuated from the atomic blast. Reasons predicted probability levels were not attained for the M-15 mine were twofold: (1) overpressures obtained in the test were lower than predicted, and (2) the mean gap on the M-15 mines used in this test was about 0.240 inch. The gap used in the static measurements on which predictions were based was only 0.106 inch. This was discovered too late to
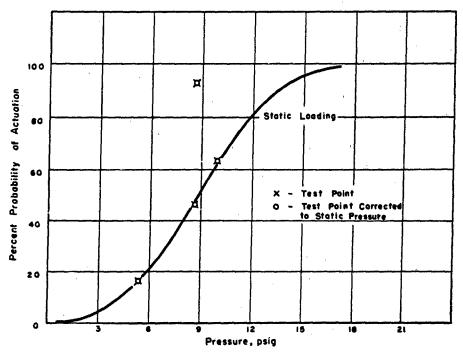
Figure 3.5 Cumulative probability distribution for US M-19 mine.

modify the test ranges for placement (Reference 1). Indications are that with the M-15 mine an increase in pressure for actuation of slightly over 3 percent would be needed for every 0.020-inch increase in gap. For the mean gap difference of 0.134 inch applicable here, a 22-percent increase in actuation pressure would be expected. This shifts the probability of actuation from 90 percent down to about 5 percent. Therefore, failure of the mines to actuate at this level appears reasonable.

The reason for the wide difference in mean gaps between samples employed for the static and atomic tests is not known. The difference may be due to variations in manufacture between different mine batches. From the available drawings of the M-15 mine, it is not possible to determine the tolerances allowed in its production.

The cumulative probability distribution for the M-15 mine is shown in Figure 3.6. This curve, based on Student's t-distribution for a sample size of 10, was determined from available static measurements and test results from the dynamic mine loading device (Reference 4). Results

40

from the atomic tests were not used although the test points are shown. The mines used in determining the curve had a mean gap of approximately 0.100 inch. Probability curves are about the same for dynamic and static loading conditions. Although the mine actuation pressure is normally lower for dynamic loading, compression of air enclosed in this mine results in a large initial reactive force which cancels the dynamic effect.

Danish M/47-I. The cumulative probability distribution for the M/47-I mine is shown in Figure 3.7. The curve was derived from the test data by the curve-fitting procedure already described. The probability that the curve should fall within expectation limits at the 99 percent
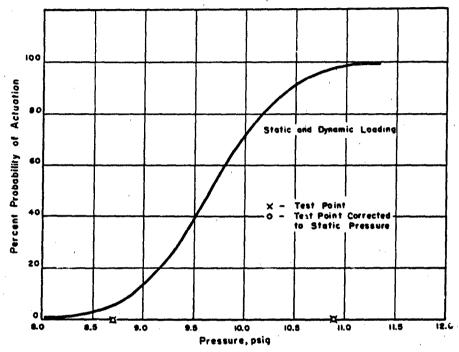
Figure 3.6 Cumulative probability distribution for US M-15 mine.

level for all three points is about 0.97. The derived curve does fall within these expectation limits, but just barely so for the point of lowest pressure.

Danish M/47-II. The cumulative probability distribution for the M/47-II mine is shown in Figure 3.8. The mine behavior was not completely static as indicated by the spread between corrected and uncorrected test points. The test point at 10.4 psi cannot be reconciled with the other two test points by consideration of expectation limits for each of the points. It was assumed to be in error or the result of an extreme sample and therefore not used in the analysis. Consequently, the curve was determined by the other two test points.

Danish M-52. The cumulative probability curve for the M-52 mine is shown in Figure 3.9. The three test points are clustered too closely together to expect an empirical fit to give satisfactory results. Thus, a reasonable value of σ/P_a based on an approximate average value for all mines was assumed. From the assumed value of σ/P_a and the centroid of the test points, the probability curve was determined by an iteration process outlined in Reference 4.

Italian CC-48. The cumulative probability curve for the CC-48 mine is shown in Figure 3.10. The curve was determined from the three test points by the procedure previously discussed for the M-19 mine.

41

SECRET
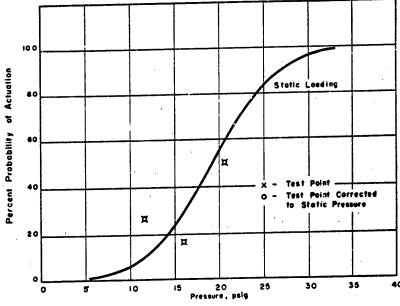
Figure 3.7 Cumulative probability distribution for Danish M/47-I mine.
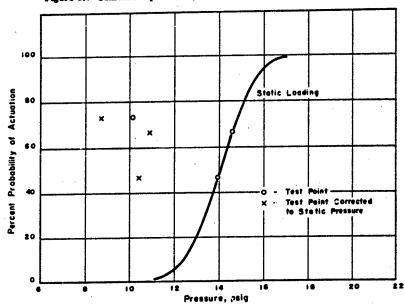
Figure 3.8 Cumulative probability distribution for Danish M/47-II mine.

SECRET
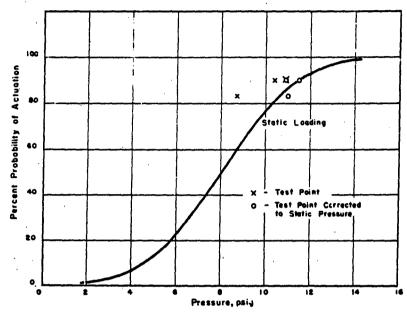
Figure 3.9 Cumulative probability distribution for Danish M-52 mine.
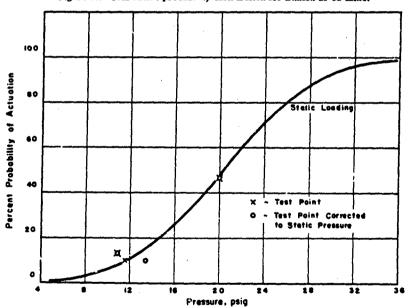
Figure 3.10 Cumulative probability distribution for Italian CC-48 mine.

43

SECRET

Italian CS-42/3. The cumulative probability distribution for the Italian CS-42/3 mine is shown in Figure 3.11. A probability curve was initially determined from the three test points by the method of least squares. However, a negative pressure was obtained at the 1-percent actuation point. Since this condition could not actually exist, it would appear that the σ determined from the three test points was too high. A more-reasonable result was obtained by discarding the lowest pressure point and determining the probability curve from the other two points.

Italian SACI. The cumulative probability distribution for the Italian SACI mine is shown in Figure 3.12. The use of all three test points in determining a probability curve gave a negative pressure at 1-percent actuation. To avoid this difficulty, the probability curve was deter-
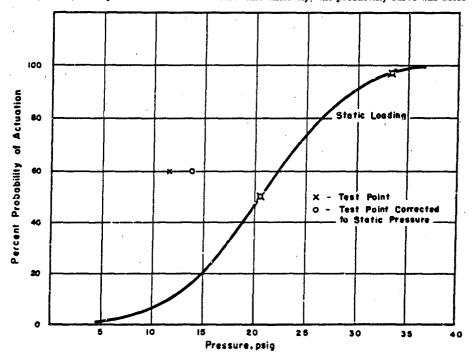
Figure 3.11 Cumulative probability distribution for Italian CS-42/3 mine.

mined from the two values at lowest pressure. This gave a reasonable value for the mean pressure and standard deviation.

Russian TMD-B. The cumulative probability distribution for the Russian TMD-B mine is shown in Figure 3.13. For the unusual distribution of the test points, the usual curve-fitting procedures would not give valid results. Hence, the curve shown was determined by assuming a reasonable value of σ/P_a and making the curve pass through the centroid of the test points.

Russian TM-41. The cumulative probability distribution for the Russian TM-41 mine is shown in Figure 3.14. Once again, the unusual arrangement of test points excluded the use of normal curve-fitting procedures. The method outlined above for the TMD-B was used.

Belgian PRB-ND-49. The cumulative probability distribution for the Belgian PRB-ND-49 mine is shown in Figure 3.15. Since the test points are clustered together, the method used for the Russian mines was used to determine this curve.

French Model 1951. The cumulative probability distribution for the French 1951 mine is shown in Figure 3.16. The curve was determined from the three test points by the usual curve-

44

SECRET
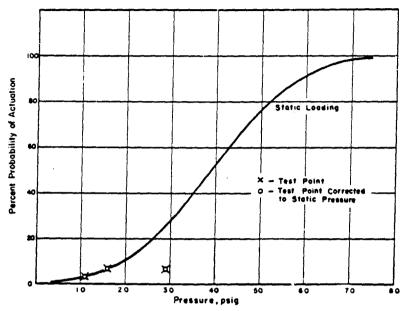
Figure 3.12 Cumulative probability distribution for Italian SACI mine.
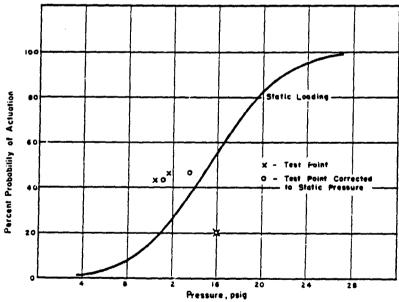
Figure 3.13 Cumulative probability distribution for Russian TMD-B mine.

45

SECRET
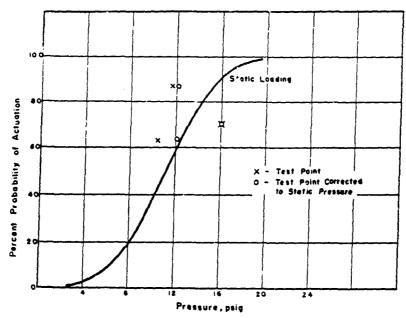
Figure 3.14 Cumulative probability distribution for Russian TM-41 mine.
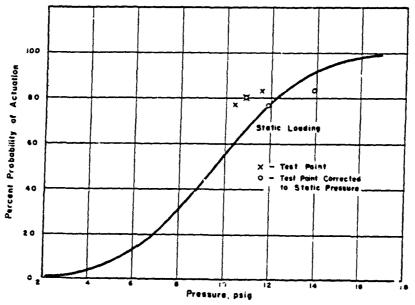
Figure 3.15 Cumulative probability distribution for Belgian PRB-ND-49 mine.

SECRET

fitting procedures. However, at the 20-psi range, none of the mines actuated. For a normal probability curve, zero actuation is reached as y approaches zero which would result in $\sigma = 0$. Accordingly, the test point for zero actuation was assumed to be the value for 1 percent actuation.

British Mark VII. The cumulative probability distribution for the British Mark VII mine is shown in Figure 3.17. The curve was determined from the three test points by the usual curve-fitting procedures. However, for the reason discussed earlier, the zero actuation test point was assumed to be the 1 percent actuation point. Although the test points were clustered together, a reasonable standard deviation was obtained by fitting a curve to the three points. Generally, this would not be true.

General. Parameters from which the cumulative probability curves were plotted are given in Table 3.5. Nearly all the parameters were determined directly or indirectly from the atomic

TABLE 3.5 STATISTICAL PARAMETERS FOR PROBABILITY DISTRIBUTION OF MINES

Mine Type	50 Percent Actuation Pressure, P_a (psi)		Standard Deviation, σ	$\dfrac{\sigma}{P_a}$	Basis for Determination
	Static	Dynamic Factor			
US M-15	9.66	1.00	0.553	0.057	Former Static and Dynamic Tests
US M-19	8.873	0.65*	3.555	0.401	Atomic Test
Danish M/47-I	19.205	0.39	5.929	0.309	Atomic Test
M/47-II	14.09	0.59	1.236	0.090	Atomic Test
M/52	8.015	0.73*	2.699	0.337	Atomic Test Assumed $\dfrac{\sigma}{P_a}$
Italian CC-48	20.263	0.65*	6.659	0.329	Atomic Test
CS-42/3	20.600	0.60	6.910	0.335	Atomic Test
SACI	38.911	0.59	15.294	0.393	Atomic Test
USSR TMD-B	15.258	0.73	5.081	0.333	Atomic Test Assumed $\dfrac{\sigma}{P_a}$
TM-41	11.093	0.94	3.694	0.333	Atomic Test Assumed $\dfrac{\sigma}{P_a}$
Belgian PRB-ND-49	9.562	0.65*	3.184	0.333	Atomic Test Assumed $\dfrac{\sigma}{P_a}$
French 1951	44.743	0.65*	11.963	0.251	Atomic Test
British Mark VII†	50.430	0.80*	15.152	0.300	Atomic Test

* Estimated.
† Data are given for arming, not actuation of mine.

test data. In addition, a column using dynamic multiplication factors is included in Table 3.5. These are multipliers used in computing pressures for 50-percent actuation under dynamic loading. The value of P_a for static conditions for any mine type is multiplied by the dynamic correction factor to determine P_a for dynamic conditions. The pressure ratios were determined from test results using the dynamic mine loading device and either the static or nuclear test results. The coefficients of variation from the nuclear test results were used to correct the dynamic results to a 50-percent actuation pressure. In all cases, the dynamic values were based on a sample size of 10 or less. Consequently, reliability was poor.

This calculation will be used when dynamic loading is probable, i.e., when devices are detonated over surfaces for which the likelihood of precursor formation is small.

A comparison of the actual test points and the test points corrected to static pressure indicates that the behavior of mines to atomic blast (this test in particular) is generally static. A few of

SECRET

Figure 3.16 Cumulative probability distribution for French 1951 mine.
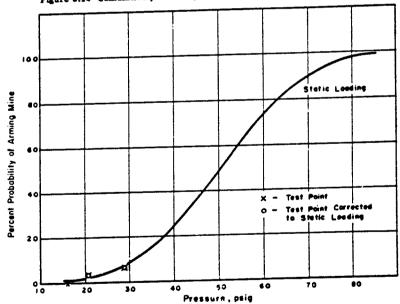
Figure 3.17 Cumulative probability distribution for arming British Mark VII mine.

48

SECRET

the mine-fields had a slight increase in percentage of actuation due to the dynamic loading effect from the precursor wave.

In static measurements, the value of σ/P_a was found to lie between 0.06 to 0.12. From atomic test results σ/P_a was found to have an average value of about 0.33 with generally only a small variation about this value. A larger value of σ/P_a was to be expected in the field test for two reasons: (1) conditions were not as closely controlled as in the laboratory, and (2) variations in soil parameters and depth of burial were present in the field test but not in the static laboratory tests where the mines were not buried. The reliability of the probability predictions could be improved if larger samples of each mine type tested by this project were tested in the laboratory for static and dynamic response.

3.2.2 Sympathetic Detonation in Live Mine Fields.

An analysis was made of the live-mine-field data to determine the increase in percent of actuation due to the mine blast pulse super-imposed upon the atomic blast pressure wave.

It was thought advisable to first determine the probability that sympathetic detonation was present. Since small samples of mines were involved, it was possible that an increase in actu-ation in the live mine fields could be due to chance variation alone. It will be assumed that when two or more adjacent mines in a live mine field detonate, sympathetic detonation is a possible cause. In a random geometric distribution of mine detonations, sympathetic detonation may have been a factor in increasing the percentage of mine detonations. In a random geometric distribu-tion of detonations, configurations favorable to sympathetic detonation will occur. If the proba-bility is small that conditions favorable to sympathetic detonation occur randomly, then some other non-random factor is responsible. It will be assumed that this other factor is sympathetic detonation. The probabilities for all random combinations of mine actuation are given in Appen-dix E. Since the likelihood for sympathetic detonation varies for different actuation patterns, the probabilities are ranked in order of favorability, with the most favorable pattern listed first.

The cumulative probability distributions and the calculated geometric mine-actuation distri-butions from Appendix E were used to establish the existence of sympathetic detonation. On the assumption that the cumulative probability distributions were correct, the probability of a ran-dom sample falling a certain distance from the curve was determined. A detailed procedure for computing these probabilities is given in Appendix E. The further the test point was above the cumulative probability curve the more favorable were conditions for sympathetic detonation.

For the majority of mine types, the various probabilities associated with random events favorable to sympathetic detonation are given in Table 3.6. No results are given for the M-15 mine, since none of the mines actuated. Results from the live TMD-B and TM-41 mines are believed to be in error, and therefore are not included. The United States replicas of the Rus-sian TMD-B and TM-41 mines use the same fuze. The detonator in the fuze has a small anvil just beneath the surface of the detonator. As the fuze actuates, a spring-loaded hammer is released to smash against the detonator. A slight misalignment, however, between the hammer and anvil will result in the detonator failing to fire. For this reason, it was thought that the test values in the live fields were low, since the Russian version of the mine has a more sensi-tive detonator for which alignment is not critical.

Table 3.6 indicates that since the probability is high for the occurrence of a random actuation pattern which is at least as favorable to sympathetic detonation as the pattern encountered in the test. Therefore, little can be learned about sympathetic detonation from considering random geometric actuation patterns.

More can be learned by consideration of random test point variations about the cumulative probability curve. The possibility of a random occurrence of points as far away from the curve as encountered in some of the live mine fields is remote. It would appear from analysis of the data in Table 3.6 that sympathetic detonation did occur in the live fields of the M-19, M/47-I, M/47-II, and Model 1951 mines, and did not occur in the M-52, CC-48, CS-42/3, SACI, PRB-ND-49, and Mark VII mine fields.

A quantitative answer to the sympathetic detonation question is difficult to obtain from the available data. A correlation was made of the percent increase in pressure with the increase

49

SECRET

in actuation between the live and inert mine fields. The results were inconsistent.

It was hoped to obtain some information about sympathetic detonation from interpretation of the live-mine-field pressure records. This could not be done due to the difficulty of distinguishing noise on the records from added mine-detonation impulses.

TABLE 3.6 PROBABILITY OF RANDOM SAMPLE BEING FAVORABLE TO SYMPATHETIC DETONATION

Mine Type	Range	Mines Detonating	Probability of Random Sample *		
			Geometric	Binomial	Combined Events
	ft				
US M-19	2,730	7	0.433	0.141	0.061
	2,870	5	0.952	0.865	0.823
	3,250	9	1.000	0.008	0.008
	5,320	10	1.000	0.000	0.000
Danish M/47-I	1,850	10	1.000	0.005	0.005
	1,990	9	1.000	0.000	0.000
	2,120	1	†	0.651	—
M/47-II	2,290	8	0.711	0.037	0.027
	2,520	7	0.433	0.568	0.246
	2,730	8	0.711	0.000	0.000
M/52	2,290	9	1.000	0.736	0.736
	2,520	9	1.000	0.582	0.582
	2,730	1	†	1.000	—
Italian CC-48	1,850	4	0.686	0.793	0.544
	2,120	1	†	0.803	—
	2,520	0	—	—	—
CS-42/3	1,600	9	1.000	0.965	0.965
	1,350	7	0.433	0.172	0.074
	2,120	2	‡	0.264	—
SACI	1,720	3	0.733	0.504	0.369
	1,990	1	†	0.016	—
	2,290	0	—	—	—
Belgian PRB-ND-49	2,120	10	1.000	0.389	0.389
	2,290	7	1.000	0.821	0.821
	2,520	0	—	—	—
French Model 1951	1,370	8	0.711	0.845	0.601
	1,500	8	0.911	0.007	0.006
	1,850	4	0.476	0.000	0.000
British Mark VII	1,720	2	‡	0.207	—
	1,850	0	—	—	—
	1,990	0	—	—	—

* Probability of a random sample being at least as favorable to sympathetic detonation as the test sample.

† Sympathetic detonation could not have occurred.

‡ Value was not computed since actuated mines were separated so that sympathetic detonation could not have occurred.

3.2.3 UIM Reading at 50 Percent Mine Actuation. The UIM reading has been useful in predicting performance of live mines under high-explosive blast conditions. However, it has not proved to be the panacea for predicting live-mine actuation under all conditions (Reference 3). For an arbitrary type of loading, the mine type to be used in conjunction with the UIM must have

similar dynamic characteristics if good reliability is to be obtained. Theoretically, under completely static or dynamic loading and for zero burial depth, the Universal Indicator reading should be reliable in predicting mine behavior irrespective of the mine characteristics, provided the appropriate UIM calibration constan. .as been determined. The UIM and the other mine involved must behave as if both were statically or dynamically loaded for the results to be correct. The qualification of zero depth of burial eliminates the effect of soil over the mine. At some depth of bur'al, depending upon the mine size, soil characteristics, etc., a bridging effect of the soil will begin to take place. For the mine types considered here, it is believed that this bridging effect will not be excessive at depths down to 6 inches.

The UIM reading for 50 percent mine actuation is given in Table 3.7 for various mines under static loading conditions. The pressure for 50 percent mine actuation was determined from the

TABLE 3.7   UNIVERSAL INDICATOR MINE READING FOR VARIOUS
MINES UNDER STATIC PRESSURE LOADING
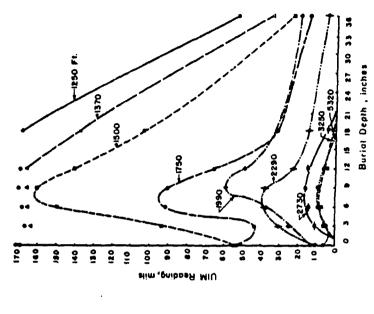
Mine Type	Pressure	UIM Reading	UIM Pressure Plate Deflection
	psig	mils	mils
US M-15	9.7	1	61
M-19	8.9	0	60
Danish M/47-I	19.2	20	80
M/47-II	14.1	1?	72
M/52	8.0	0	57
Italian CC-48	20.3	22	82
CS-42/3	20.6	22	82
SACI	38.9	59	119
USSR TMD-B	15.3	14	74
TM-41	11.1	5	65
Belgian PRB-ND-49	9.6	1	61
German TMi-43	46.9	83	143
French Model 1951	44.7	76	136
British Mark VII	50.4	98	158

appropriate cumulative probability curve and the UIM reading for that static pressure (Reference 4). Figure 3.18 shows how well the test data fits the curve developed from laboratory tests for UIM deflection versus pressure. Agreement is good at zero depth of burial.

For other depths of burial, the data in Appendix F can be employed to compute UIM reading versus pressure. However, even at shallow burial depths, factors come into play which result in an increase in UIM reading with depth. Possible causes for this phenomenon are presented later but the final outcome is to reduce the reliability of prediction from UIM readings.

3.3 DEPTH-OF-BURIAL STUDY

3.3.1 Results and Discussion. The variation of UIM readings with depth of burial for a given range is shown in Figure 3.19. From the figure, the following observations can be made: (1) at overpressures equal to or greater than 60 psi and depths of burial less than or equal to 18 inches, the maximum UIM reading was obtained (at the maximum UIM reading, the Belleville springs of the meter have been completely flattened and no higher reliable reading can be obtained); (2) there was a significant increase in pressure plate deflection from 0 inches of burial to depths of burial between 6 and 9 inches with a maximum response occurring somewhere between 6 and 9 inches. This behavior was observed for overpressures less than about 45 psi. Contrary to observations made for the mine field clearance project of Operation Upshot-Knothole (Reference 3), this in-

51

SECRET

Figure 3.19 UIM reading versus mine burial depth for different ranges from ground zero.
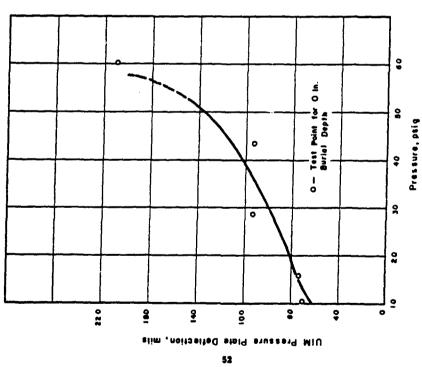
Figure 3.18 Pressure-plate deflection of UIM versus pressure for static loading conditions.

crease was appreciable. Whether or not this phenomenon occurs for overpressures greater than 45 psi cannot be determined, since maximum UIM readings occurred at the high pressures of 60 and 76 psi.

Figures 3.20 through 3.26 are included to demonstrate the relationship between the UIM response with overpressure for fixed depths of burial. A straight line was fitted to the points for each depth of burial. UIM readings above 160 mils were usually neglected as being unreliable.
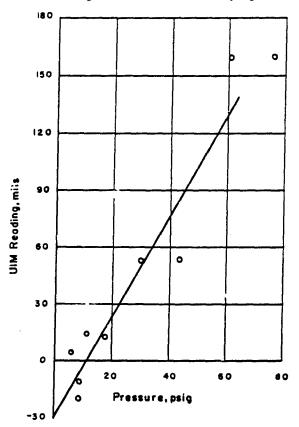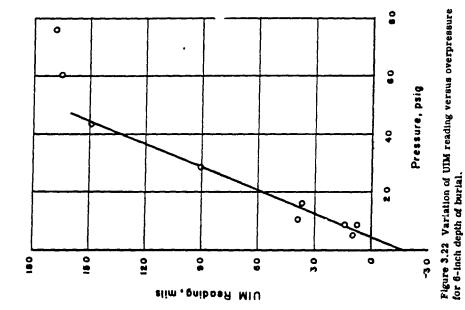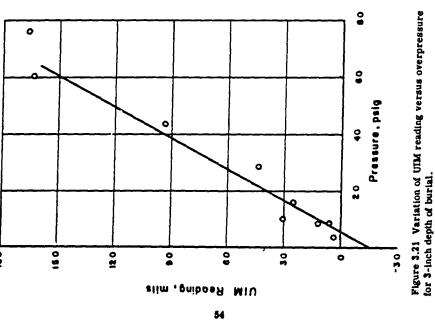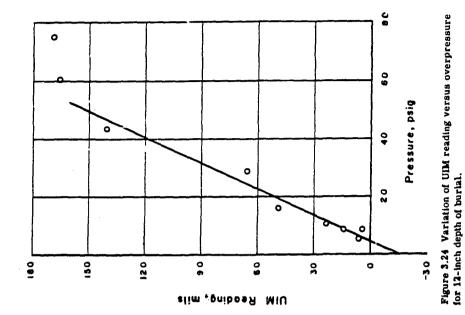
Figure 3.20 Variation of UIM reading versus overpressure for 0-inch depth of burial.
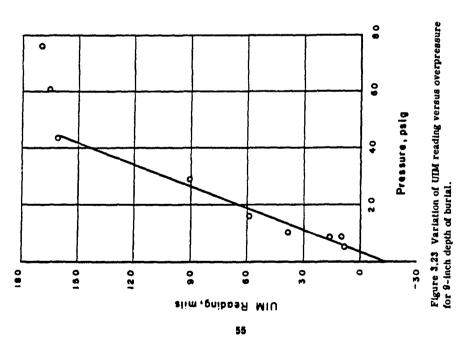
All UIM readings were corrected to a 60-mil gap by assuming a linear relation existed between the UIM reading and the gap and fitting a straight line to the data by the method of least squares.

Reason for the extent of the increase in UIM response with burial depth is not obvious. The use of one-degree-of-freedom theory to predict UIM deflection under a gradually applied load for a depth of 6 inches gives a maximum deflection 20 percent greater than the deflection at 0 inches of burial for a statically applied pressure (Reference 3). However, at the 1,500-foot range and 6-inch burial depth, the actual increase above static deflection is about 65 percent. In an effort to resolve this dilemma, an analog computer was employed to apply linear two-degrees-of-freedom theory to predict the mine behavior (Reference 4). The soil over the mine was considered as a concentrated mass elastically coupled to the pressure plate. The results

53

SECRET

Figure 3.22 Variation of UIM reading versus overpressure for 6-inch depth of burial.

Figure 3.21 Variation of UIM reading versus overpressure for 3-inch depth of burial.

54

SECRET

Figure 3.24 Variation of UIM reading versus overpressure for 12-inch depth of burial.

Figure 3.23 Variation of UIM reading versus overpressure for 9-inch depth of burial.

55

SECRET

Figure 3.26 Variation of UIM reading versus overpressure for 36-inch depth of burial.

Figure 3.25 Variation of UIM reading versus overpressure for 18-inch depth of burial.

56

were in good agreement with the theoretical results from one-degree-of-freedom theory, but did not explain the unexpectedly large UIM deflections

Since linear theory does not explain this phenomenon, it seems necessary to consider other effects. From experimental tests on the TMi-43 mine using the dynamic mine loading device, it was observed that the second (reflected) pressure wave often actuated the mine even though the peak pressure was 25 percent lower than the peak pressure for the first wave. The reason for this was attributed to weakening plastic deformation (permanent set) of the pressure plate by the first wave. Weakening through plastic deformation was also indicated from cyclic loading tests made during static force-deflection measurements. For nuclear air blasts like Shot Priscilla there would be a repeated loading on the mine due to the precursor wave. This may be a contributing factor in the large UIM readings.

Another reason for this phenomenon may be nonlinear behavior of the soil itself. The modulus of deformation of the soil at the test site is known to increase nonlinearly with the magnitude of the applied pressure. From earlier test work using the loading device (Reference 4), it was found that the earth pressure was increased to more than double the peak blast pressure because of reflection from a rigid body in the soil. The two-degrees-of-freedom linear theory predicts this. However, it was observed that the second pressure wave, occurring about 0.15 second after the first reflection, produced an earth pressure equal to the earth pressure from the first wave despite the fact that the amplitude of the second wave was only about 75 percent of the amplitude of the first. It would appear that this pressure increase could be due only to an increase in soil deformation modulus with depth after passage of the first wave. In order for this phenomenon to occur under atomic blast conditions, the modulus would have to change with depth during load application since the modulus would initially be independent of depth at shallow burial depths. The mechanism by which a modulus increase with depth could occur during loading may be envisioned by considering the sloping front of the wave as made of a series of little step waves. As each little pressure wave transmitted through the soil contacts the pressure plate, it is reflected, causing an increase in pressure above the pressure plate. This in turn increases the soil density since the soil is inelastic, and therefore the modulus of deformation increases. If it is assumed that the increases in modulus increase the pressure, an appreciable variation of modulus with depth will be detectable by the time the peak pressure is attained, and therefore deflection increases.

3.3.2 Prediction from UIM Data of Mine Responses at 36-inch Depth.
Since the use of the UIM for predicting live-mine detonation under arbitrary loading conditions should be limited to mines with characteristics similar to the UIM, application of UIM data to predict behavior of other mine types in general is fraught with danger. However, because no data is available on mine behavior at burial depths below about 6 inches, it would seem worthwhile to attempt to predict mine behavior at deeper burial depths from the available UIM data.

Predictions are made of the 50-percent actuation point for the various mines of this test when buried 36 inches deep. It is believed that at this deep burial depth, all mines will display about the same natural frequency, so dynamic behavior should be about the same for the UIM as for other mines. If the mine pressure-plate area and mine deflection for actuation corresponds with that of the UIM, then it is thought that the prediction should be reasonably accurate. For most mines these last two characteristics are not the same as those for the UIM and thus some error is to be expected.

On the basis of these assumptions, predicted pressures for 50-percent actuation of the various mines at 36-inch burial depth are given in Table 3.8. Values were determined from a straight-line fit of UIM reading versus pressure at the 36-inch depth of burial.

3.3.3 Correlation of UIM and TMi-43 Mine Test Results.
Characteristics of the UIM and TMi-43 mine are similar. Therefore, it is logical to expect that the UIM data can be employed to adequately predict TMi-43 mine detonation for a wide variety of conditions.

57

SECRET

The following procedure was used in applying UIM data to the prediction of TMi-43 mine behavior at different burial depths:

1. A static UIM reading of 83 mils was assumed for the TMi-43 mine.
2. Using this value, the corresponding pressure was determined from the straight-line fit

TABLE 3.8 PRESSURE FOR 50 PERCENT MINE
ACTUATION AT 36-INCH BURIAL
DEPTH

Mine Type	Pressure, psig
US M-15	15.2
M-19	17.1
Danish M/47-I	39.1
M/47-II	30.3
M/52	13.8
Italian CC-48	41.4
CS-42/3	41.4
BACI	82.2
USSR TMD-B	32.5
TM-41	23.6
Belgian PRB-ND-49	18.2
German TMi-43	108.7
French Model 1951	100.9
British Mark VII	125.2

on the UIM reading versus pressure curve for the particular burial depth. This pressure corresponded to the overpressure to actuate 50 percent of the TMi-43 mines.

3. A value of $\sigma/P_a = 0.12$ was assumed for the TMi-43 mine. This value was double the value obtained during static-loading tests in the laboratory and appears reasonable for use with the test data.

TABLE 3.9 COMPARISON OF TEST RESULTS AND PREDICTED
VALUES BASED ON UIM TEST RESULTS FOR
TMi-43 MINE

| Overpressure | Percent Actuation | | Burial Depth | Range |
	Predicted	Test		
psig			in	ft
76	Above 99	100	0	1,250
66.5	Above 99	100	0	1,370
43.6	77	100	0	1,500
76	Above 99	100	3	1,250
66.5	Above 99	100	3	1,370
43.6	96	100	3	1,500
76	Above 99	100	6	1,250
66.5	Above 99	100	6	1,370
43.6	Above 99	100	6	1,500
76	Above 99	100	9	1,250
66.5	Above 99	100	9	1,370
43.6	Above 99	100	9	1,500
76	Above 99	100	12	1,250
66.5	Above 99	100	12	1,370
43.6	Above 99	100	12	1,500
76	Above 99	100	18	1,250
66.5	Above 99	100	18	1,370
43.6	81	50	18	1,500
76	Less than 1	0	36	1,250
66.5	Less than 1	0	36	1,370
43.6	Less than 1	0	36	1,500

4. The percentage of TMi-43 mines that should actuate at the test overpressure was determined by normal probability theory.

A comparison between the predicted and actual mine actuation is given in Table 3.9. The UIM data satisfactorily predict TMi-43 mine actuation for the various depths except at the 43.6-
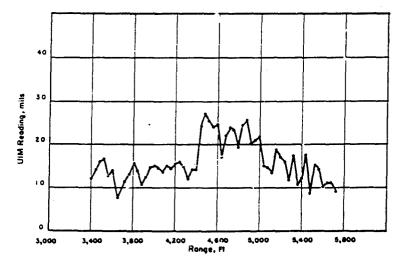
Figure 3.27 Variation of UIM reading with range.
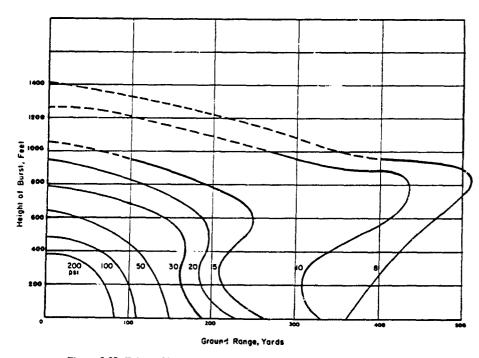
Figure 3.23 Height of burst versus range for 1 kt and a given overpressure.

59

SECRET

psi overpressure and zero burial depth. The reason for this discrepancy is not definitely known. Perhaps the heat wave from the explosion weakened the mine. In several depths of burial fields nearest ground zero, the heat was sufficient to burn the paint off the pressure plates of the mines at the surface.

3.4 CHANGE FROM STATIC TO DYNAMIC PRESSURE WAVE

Results from the special fields of UIM's placed between ranges of 3,250 to 5,320 feet are shown in Figure 3.27. These mines were used to determine if an appreciable increase in deflection occurred as the pressure wave shape changed from a gradual to a rapid pressure rise over the intial portion of the wave. Figure 3.27 indicates that a 20-percent increase in deflection does occur at about 4,000 feet. A similar increase in actuation at 4,530 feet occurred for the M-19 mine.

These two occurrences strongly indicate that there was an increase in dynamic response due to a sharpening of the wave front. However, pressure data were lacking beyond 3,250 feet so no quantitative correlation of this phenomenon with theory could be made.

3.5 HEIGHT OF BURST FOR MAXIMUM CLEARANCE

In view of the speculation in previous mine field clearance operations about an optimum height of burst for maximum ranges of clearance, it was considered advisable to include an overpressure curve extracted from Reference 6 (Figure 3.28). From the graph, determination of the range of an overpressure for a given height of burst is quite simple.

Cube-root scaling should be applied to the results for 1 kt to extrapolate for various yields (Reference 6). Figure 3.28 is only for soil conditions similar to those at the NTS.

SECRET

Chapter 4
CONCLUSIONS and RECOMMENDATIONS

4.1 CONCLUSIONS

1. Current procedures are reasonably accurate for predicting mine actuation under nuclear explosions through the use of static actuation pressures along with information on the shape of the pressure wave.

2. Sympathetic detonation occurs for some mine types for the normal spacing between live mines in standard mine-field patterns. No quantitative explanation can be given for this occurrence.

3. UIM readings increase with depth of burial to a maximum value at 6 to 9 inches of cover. The extent of the increase can not be explained by application of the linear one-degree-of-freedom spring-mass theory, and is attributed to nonlinear behavior of either the mine or soil cover or both.

4. Conclusions for four subprojects by Picatinny Arsenal, DOFL, Chemical Warfare Laboratory, and the United Kingdom are included in the respective appendices devoted to those projects.

4.2 RECOMMENDATIONS

1. Mine actuation theory should be extended to include nonlinear soil effects in order that mine actuation may be predicted at depths greater than 6 inches.

2. A field manual should be prepared for mine clearance by nuclear blast for known mine types over a practical range of environmental conditions. This should include a summary of the expected changes in wave shapes as the burst environment varies, with specific remarks on the relative prominence of the precursor.

3. No extensive efforts should be undertaken to determine a quantitative explanation of sympathetic detonation because: (1) sympathetic detonation is not a major factor in determining the percentage of mines actuated, and (2) the mine types affected by sympathetic detonation were generally those most easily cleared by blast. This is most significant since mine design is presently concerned with the development of mines resistant to clearance by nuclear blast.

4. Further testing of clearance of conventional-design, pressure-actuated mines by nuclear blast is unnecessary for the following reasons: (1) the techniques for prediction of actuation are sufficiently refined to make a reliable prediction after an adequate sample of mines is examined by laboratory analysis: i.e., pressures for 50-percent actuation can be determined for various types of loading and actuation probability curves can be developed assuming $\sigma/P_a = 0.33$ for the data under field conditions; and (2) present methods for predicting P_t curves are quite accurate. Nuclear field tests might be required for mine designs not amenable to laboratory analysis.

5. Laboratory testing of larger samples of the mines should be undertaken in order to improve the reliability of the actuation prediction curves.

6. Recommendations for the four subprojects are included in the separate appendix devoted to each subproject.

61

SECRET

Appendix A
PROTECTION of PRESSURE-ACTUATED
MINES AGAINST NUCLEAR BLAST

The purpose of the test was to evaluate the effectiveness of two experimental designs in providing pressure-actuated mines with protection against blast effects of nuclear explosions. The two designs were code named High Hat and Partner.

High Hat was an auxiliary mechanical device designed for use with standard pressure-actuated antitank mines and required no modification of the mine or fuze. For this test, High Hat was adapted to the M-19 mine and designed to provide protection against overpressures up to 70 psi.

The test was to determine whether the design provided reduction of functioning under blast pressures, as compared to unprotected mines, and to find the magnitude of pressure that would cause the protection to fail.

Partner was a two-mine system in which pressure-actuated, mechanically initiated mines were modified to provide electrical initiation. Two mines with identical fuzes were electrically coupled in a manner such that actuation of either mine independently would function the mine in a normal manner, but application of pressure to both mine plates simultaneously would prevent either from functioning.

The purpose of this test was to determine the functioning characteristics of the system. Means were provided by which possible causes of failure could be tested.

A.1 BACKGROUND

The test described was initiated to provide information for a feasibility study being conducted by Picatinny Arsenal (PA) under Ordnance Project TA3-5926. The purpose of the study was to develop new pressure-actuated mines and accessories with reduced vulnerability to the effects of nuclear explosions and to provide standard pressure-actuated mines with similar protection.

Preliminary testing of High Hat was conducted to determine the effect of burial depth on the ability of the design to function when actuated by a tank. Models were placed in 15-inch-diameter holes in dry, sandy soil. The holes were sloped 45 degrees to prevent bridging. It was found that functioning occurred consistently under full track coverage with a burial depth down to 4 inches. An M4 Sherman tank of approximately 35 tons was used for the tests.

No tests were conducted on the functioning of Partner under a tank, because the design did not change the functioning characteristics of the M-19 mine to which it was adapted. However, complete laboratory checks were made to insure that the electronic circuitry used in the design functioned according to specifications.

The two designs tested were proposed means of providing standard pressure-actuated antitank mines with protection against the blast effects of nuclear detonations. Both designs were adapted to the M-19 mine, although their use is not limited to that mine.

A.1.1 High Hat. High Hat consisted of two cylinders. As adapted to the M19 mine, the larger cylinder had an outside diameter of 9.5 inches and was 1 inch high. To this cylinder was welded a circular cover with four annular slots; the complete unit thus formed was called the base. A second cylinder, called the hat, was 7.6 inches in diameter and 1.7 inches high. Four notches were cut in the hat, so that it would fit into the slots in the base. The base and hat and the manner in which they fit together are shown in Figures A.1 and A.2.

Within the small area occupied by a mine, the pressures from the blast wave are experienced almost simultaneously (within 1 msec) by all points. Since the force experienced by the mine fuze is proportional to the area of the pressure plate, the force can be reduced by changing the size of the plate or by partially covering it. The latter is the function of the base of the High Hat. The base is placed over the pressure plate resting on the static portion of the mine. Thus, the pressure acting on the base is transmitted to the mine body, not the fuze.

The cylindrical hat fits into the slots in the base and rests directly on the pressure plate. When in this position, the hat is raised slightly by the pressure plate, which protrudes up under the base of the High Hat. This can be seen in Figure A.3. When pressure is applied, the hat is forced down, depressing the pressure plate and functioning the fuze. Because only the pressure acting on the comparatively small area of the hat is transmitted to the fuze, approximately 70 psi is required to cause functioning. By comparison, an unprotected M-19 mine can be caused to function under about 9 psi.

A tank, however, does not exert a uniform ground

62
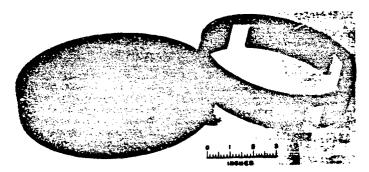
Figure A.1 High Hat, showing the base and hat separated.
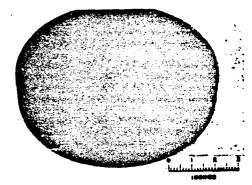
Figure A.2 High Hat, showing base and hat assembled.
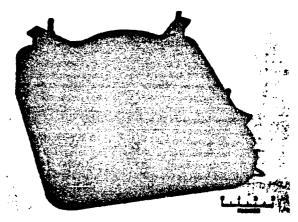
Figure A.3 High Hat mounted on an M-19 mine. Four
brackets prevent base of High Hat from slipping.

63

SECRET

pressure. The tank track is not deformable, as is a pressure wave. When a tank passes over a High Hat, the earth around and in the center of the hat tends to push aside and compact. This leaves the hat to bear the major portion of the force exerted by the tract above it. When the High Hat is buried 4 inches or less, this force is sufficient to function the fuze.

A.1.2 Partner.

The partner system utilizes the fact that two mines buried the standard 18 feet apart will both be subjected to the blast wave within a short time. For example, if it is assumed that the blast wave travels at only 1,000 ft/sec and that the mines are 20 feet apart, it will take only 0.02 second for the shock front to move from one mine to the other if they are placed along a line radial to the point of blast. Actually, in regions where overpressures of sufficient strength occur to function the mine, the shock front moves more rapidly. Thus, if the mine pair are electrically coupled so that depression of both pressure plates within 0.5 second will prevent functioning of either, the pair is insured of protection from overpressure effects. In the Partner system, a resistance-capacitance bridge circuit is used to accomplish the coupling.

For this test, Partner was adapted to the M-19 mine. The method of modification provided a means for determining not only the success or failure of the protective system but whether or not the mines, if unprotected, would have functioned.

The physical modification of the mines is shown in Figure A.4. A plunger assembly is screwed into the detonator fitting of the mine fuze. When the fuze is functioned, the firing pin strikes the plunger, which causes the microswitch assembly mounted on the bottom of the mine to change from its normally closed position to the normally open position. The electrical circuitry is located in a chassis mounted on the bottom of the mine. Both mines of the pair contain identical switch assemblies and circuitry and are connected electrically by a four-conductor cable.

The microswitch assembly contains five single-pole, double-throw microswitches, which are ganged to function simultaneously when the plunger is depressed. These switches correspond to S_1, S_2, S_3, S_4, in the circuit diagram of Figure A.5. Switch S-5 is physically located in the other mine of the Partner pair, and the corresponding switch of the second mine is wired to the fifth pole of the microswitch assembly in the first mine.

When the pressure plate of only one mine is depressed, the switches close. Capacitors C_1 and C_2, which have been charged to equal voltages by the battery, are connected to the two resistance loops of the circuit. A current i_1 then flows through Loop I in the direction shown in Figure A.5, charging the firing capacitor, C_3. The current i_2 in Loop II is zero, because Switch S-5, located in the other mine, is open. When C_3 charges to the firing voltage of the glow tube (gas-discharge diode) the tube fires

(essentially changes from an open circuit to a short circuit) and an electric detonator is set off by the discharge of C_3.

Resistor R_1 provides a time delay of 0.5 second after switches S_1 and S_2 close before C_3 charges sufficiently to fire the detonator. The delay insures protection of the mine pair when both plates are not depressed at exactly the same instant.

When both mines of the pair are functioned within 0.5 second, neither detonator is set off. Switch S-5 in both circuits is closed. Capacitor C_1 and C_2 have equal values, as do resistors R_1 and R_2. Therefore, the circuit is a balanced bridge with current i_1 in Loop I equal in magnitude but opposite in direction to current i_2 in Loop II (See Figure A.5). The currents in the two loops cancel, and capacitor C_3 does not charge.

The adaptation of the Partner system to the M-19 mine, as used in this test, prevented functioning of the two mines of the pair when both experienced the influence of the blast wave from a nuclear detonation; however, both mines were permanently sterilized, and neither would subsequently function under a tank. The M-19 mine fuze has two Belleville springs, a main load-bearing spring and a smaller snap-through spring, which normally drives the firing pin into a percussion detonator. The small spring does not return to its original position when the mine plate is released, after having been depressed. In order to adapt the mine to the Partner system, it would be necessary to redesign the fuze, replacing the snap-through spring with a microswitch. Then depression of the plate would directly operate the microswitch, and the fuze would return to its original position when released. Thus, after the pressure wave of a blast had passed, both mines would be capable of functioning under a tank (Figure A.4).

The mines used in this test did not have the modifications just described. There were two reasons for this: (1) Because it was desired to test only the ability of the Partner system to provide protection against blast effects, it was considered more expedient to design the small plunger assembly than to modify the fuze. (2) By using an unmodified fuze, it was possible to tell by examination of the snap-through Belleville spring whether or not the fuze had functioned. Thus, if the fuzes in both mines of a Partner pair had functioned, and neither indicator detonator had fired, then it would be known that the protection system had worked properly.

A.2 PROCEDURE

A total of 43 mines, 25 High Hats and 18 Partners (9 pairs), were planted in Frenchman Flat in the Project 6.1 inert mine field. The experimental layout is shown in Figure A.6. Holes were dug with a power auger mounted on a 2½-ton truck. The holes were 24 inches in diameter and had flat bottoms and perpendicular sides.

SECRET
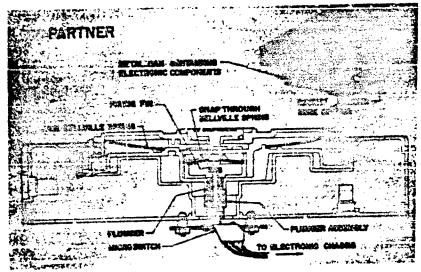
Figure A.4 Cross-sectional view of an M-19 mine, showing the modifications that were made to adapt it to the Partner system.
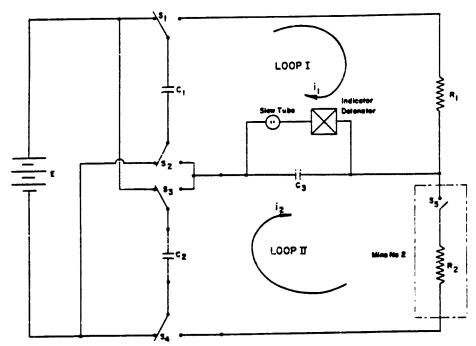
Figure A.5 Circuit diagram showing the circuitry used in the Partner system.

All results were recorded on a go or no-go basis. That is, it was noted whether or not each prototype had functioned. Remarks as to the condition or physical position of the mines and modifications as found after the test were noted where such notation could give an indication of the reasons for success or failure.

A.2.1 High Hat. High Hat was tested at three overpressure levels.

Five models were placed at 21 psi. This was one station higher than that at which 90-percent functioning could be expected for an unprotected M-19 mine. If the mines functioned at this station, it was to be concluded that no protection had been afforded by High Hat.

Five models were placed at 40 psi. This was in intermediate point between the no-protection-afforded station and that station at which failure of protection was expected (70 psi).

Five models were to be placed at 70 psi, because analysis had shown that the presented area of High Hat was such that overpressures of 70 psi or greater would cause it to function when used with an M-19 mine. It was desired to determine the actual functioning overpressure in this test. Because it had been found that the M-19 mine functions over a range of pressures, it was necessary to place the test models of High Hat at pressures somewhat greater than, and less than the expected functioning level. It was desired that five prototypes per station be placed at 85 psi, 70 psi, and 55 psi. Because the greatest overpressures available at the Project 6.1 test site were 60 psi, 15 models of High Hat were modified to give greater presented area, so that they would simulate the effects of higher pressures when placed at the stations available. The actual placement of these modifications is indicated in Table A.1.

The High Hats were placed in holes as shown in Figure A.7. A cloth cover was placed over each High Hat to prevent sand from causing binding. The tops of the hats were 3 inches below ground level, and the holes were filled flush with the ground.

A.2.2 Partner. The Partner pairs were arranged in patterns, three pairs in each pattern, as shown in Figure A.8. Pairs were arranged in this manner to determine the effects of orientation to ground zero on the simultaneous operation of the two mines. Furthermore, it was known that a strong electromagnetic signal was given off by a nuclear detonation. It was felt that this signal might be picked up by the connecting cables and affect the electronic circuitry. By placing the Partner pairs in the patterns described, the effect of electromagnetic pickup (if any could be noticed) could be related to orientation.

Pattern 1 was placed at the 50-psi station to test performance of the system under high overpressure. Patterns 2 and 3 were placed at the 21-psi station to determine whether the partner system afforded any improvement over planting the mines unprotected. The exact location of these patterns is shown in Figure A.6.

Four control circuits, containing circuitry duplicated to that used in the Partner chassis (except for the omission of the microswitch and battery) were planted in the mine field. Two control circuits were placed in Pattern 1 and one each in Patterns 2 and 3. These controls were devised to check whether or not the electromagnetic field created by the blast was sufficient to cause the sensitive electric detonators used in the cirucitry of Partner to function. The control circuits were buried 5 inches deep.

The mines were placed in the holes as shown in Figure A.9. Pieces of wood 2 by 4 by 13 inches were placed under three edges of the mine to prevent the blast pressure from crushing the metal chassis. Cables connecting the two mines of each pair were buried in 6-inch trenches. The tops of the mines were 5 inches below ground level, and the holes were filled in flush with the ground.

A.3 RESULTS AND DISCUSSION

Overpressure levels were selected to yield the maximum amount of information from the limited number of test items available. Results of the pressure gages located in the Project 6.1 mine field showed that the measured overpressures differed considerably from the predicted, particularly at the high-overpressure stations. At the 60-psi station, the measured pressure was about 25 percent high; at the 50-psi station, the pressure was about 20 percent high. The 40-psi station was only 8 percent high, and the 21-psi station was 24 percent low. Partially because of the pressure differences, the results were not as conclusive as it had been hoped they would be.

A.3.1 High Hat. The results of the High Hat test are shown in Table A.2. Predicted and measured overpressures are shown for comparison. As stated in Section A.2.1, 15 High Hats were modified by an increase in the presented area of the hats in order to simulate higher overpressures. The pressure simulated by any of these models is equal to the actual pressure multiplied by the ratio of the modified area to the unmodified area. Because the actual overpressures at the stations where these models were placed were higher than predicted, the simulated pressures were also higher. The actual simulated pressures are listed in the table.

All mines with modified High Hats were actuated. From pretest calculations, it could be expected that these would function because of the higher-than-predicted simulated pressures. However, from these same calculations, it could be expected that at the unmodified models at the measured overpressure of 43.6 psi would not function. Of the five High Hats located at this station, three failed to protect the mines. None of the mines functioned at 16 psi. This would indicate

66

SECRET
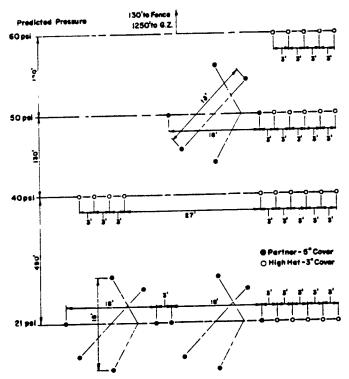
Figure A.6 Layout of experimental mine field.
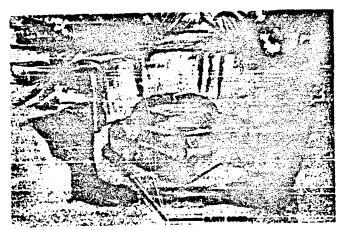
Figure A.7 Sectioned view of High Hat in place before hole is filled.

67

SECRET

TABLE A.1   PLACEMENT OF HIGH HAT

Number of High Hats	Predicted Overpressure Stations psi	Modified to Simulate Over- Pressures of psi
5	21	No Modifications
5	40	No Modifications
5	40	55
5	50	70
5	60	85
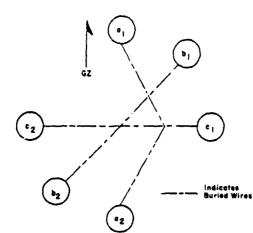
Figure A.8 Partner pattern showing orientation to ground zero. The cable between Mines a_1 and a_2 was staggered to prevent the blast wave from blowing the earth out of the length of the trench. Though the cables cross physically, they are not in contact electrically.

Indicates Buried Wires

Figure A.9 Sectioned view of Partner in place before hole is filled.

68

SECRET

that the High Hats, as now designed, can insure protection to some value of overpressure less than 43.6, which seems to be about a 50-percent point. However, even if insurance of protection extends only to 35 or 30 psi, these pressures are considerably higher than the unprotected mine could survive. Furthermore, by reducing the presented area of the High Hats through redesign, it should be possible to raise the level of protection.

The results of this test indicate that, although High Hat did not perform as well as expected, the

The circuitry in both mines should have worked properly when tested in the laboratory after the shot, indicating that the mines would be in condition to function when actuated by a tank. Fulfillment of all three requirements would indicate success of the Partner system.

None of the detonators in the control circuits planted in any of the Partner patterns fired; therefore, it is known that electromagnetic pickup did not affect the circuitry in the mines.

All three Partner pairs (all of Pattern No. 1)

TABLE A.2   HIGH HAT RESULTS

Mine Number*	Distance From Ground Zero	Predicted Overpressure	Measured Overpressure	Pressure Simulated by Modification at Predicted Overpressure	Pressure Simulated by Modification at Measured Overpressure	Condition of Mine After Test
	feet	psi	psi	psi	psi	
1	1,250	60	78.0	85	108	Functioned
2	1,250	60	78.0	85	108	Functioned
3	1,250	60	76.0	85	108	Functioned †
4	1,250	60	78.0	85	108	Functioned
5	1,250	60	76.0	85	108	Functioned
6	1,370	50	60.5	70	86	Functioned
7	1,370	50	60.5	70	86	Functioned
8	1,370	50	60.5	70	86	Functioned
9	1,370	50	60.5	70	86	Functioned
10	1,370	50	60.5	70	86	Functioned
12	1,500	40	43.6	55	62	Functioned
14	1,500	40	43.6	55	62	Functioned
16	1,500	40	43.6	55	62	Functioned
18	1,500	40	43.6	55	62	Functioned
20	1,500	40	43.6	55	62	Functioned ‡
11	1,500	40	43.6	§	§	Not Functioned
13	1,500	40	43.6	§	§	Functioned
15	1,500	40	43.6	§	§	Functioned
17	1,500	40	43.6	§	§	Functioned
19	1,500	40	43.6	§	§	Not Functioned
21	1,990	21	16.0	§	§	Not Functioned
22	1,990	21	16.0	§	§	Not Functioned
23	1,990	21	16.0	§	§	Not Functioned
24	1,990	21	16.0	§	§	Not Functioned
25	1,990	21	16.0	§	c	Not Functioned

* Refer to the numbers placed above each mine in Figure A.6.
† Neville spring had not snapped through; the plastic cup which holds ... ng had broken off, indicating that the mine had received enou... ...ure to operate, but had malfunctioned.
‡ Mine had mo... ...er the blast and was found partially exposed.
§ These mines had unmodified High Hats.

design offered considerable improvement over the unprotected M-19 mine.

A.3.2 Partner. The results of the Partner test are summarized in Table A.3. In order for the Partner pair to have worked as desired, the following conditions should have occurred: (1) The fuzes in both mines of the pair should have functioned, indicating that the mines, if unprotected, would have been set off. (2) The electric detonators in both electronic chassis should not have fired, indicating that the mines were protected by the Partner system. (3)

placed at the measured overpressure of 60.5 psi fulfilled the above conditions.

At 16 psi in Pattern 2, only pair B_1-B_2 met the three conditions. In pair C_1-C_2, neither mine fuze functioned. This indicates neither success no failure of the Partner system, because it was given no chance to protect the mines. These two mines survived the blast pressure without protection. No information was gained from this pair. Pair A_1-A_2 points out both a general disadvantage of the Partner design and a failure of one of the mines of the pair. The fuze in Mine A_1 functioned; that in Mine A_2 did not.

SECRET

The pressure to which these mines were exposed was that at which 5 [?]-percent functioning of M-19 mines could be expected. At this pressure, and for lower pressures (down to the level at which no functioning of unprotected mines would occur), there is the danger that one mine plate of the pair will be depressed and the other will not. When this occurs, Partner will offer no protection, and the first mine will be cleared by the blast. At higher pressures, where it is insured that both mine plates will be depressed, the Partner system will prevent clearance by the

the mine. The circuitry, nevertheless, did not work properly, and this is a failure of the Partner system. One possible explanation of the failure can be offered.

It was noticed that the detonator in this mine fired in less than the designed 0.5 second when the circuitry was tested, indicating that the gas diode in the circuit (see Figure A.5) fired at less than the designed voltage. If this occurred during the nuclear test, the energy transmitted to the detonator may not have been enough to fire it. However, this may have made the detonator more sensitive, so that it would fire when

TABLE A.3 PARTNER RESULTS

Pattern Number*	Mine Number†	Orientation of Partner Pair to Radial Line From Ground Zero	Predicted Overpressure	Measured Overpressure	M-19 Mine Fuze was Functioned By the Blast Pressure	Electric Detonator in Partner Chassis Had Fired	Partner Chassis Functioned Normally When Reset in the Laboratory After the Atomic Test
			psi	psi			
1	a_1	radial	50	60.5	yes	no	yes
1	a_2	radial	50	60.5	yes	no	yes
1	b_1	45 degrees	50	60.5	yes	no	yes
1	b_2	45 degrees	50	60.5	yes	no	yes
1	c_1	tangential	50	60.5	yes	no	yes
1	c_2	tangential	50	60.5	yes	no	yes
2	a_1	radial	21	16.0	yes	no	?‡
2	a_2	radial	21	16.0	no	no	yes
2	b_1	45 degrees	21	16.0	yes	no	yes
2	b_2	45 degrees	21	16.0	yes	no	yes
2	c_1	tangential	21	16.0	no	no	not tested
2	c_2	tangential	21	16.0	no	no	not tested
3	a_1	radial	21	16.0	yes	no	yes
3	a_2	radial	21	16.0	yes	no	yes
3	b_1	45 degrees	21	16.0	yes	no	yes
3	b_2	45 degrees	21	16.0	yes	no	yes
3	c_1	tangential	21	16.0	yes	no	yes§
3	c_2	tangential	21	16.0	no	no	yes

* These refer to the pattern numbers on Figure A.6.
† These refer to the mine numbers on Figure A.6.
‡ When tested, the detonator seemed to fire in considerably less than 0.5 seconds, however the firing time was not measured with a chronograph.
§ A connecting plug inside the chassis was found disconnected. It is not known whether this occurred before or after the test.

blast. However, there is the range of pressures just described in which this system offers little protection.

As stated above, Mine A_1 is considered to have been cleared by the blast. The fuze of only this mine of the pair functioned; therefore, the electric detonator in the Partner chassis should have fired, just as it should when a tank functions one mine of a pair. However, the detonator did not fire. The reason for this is not apparent from the posttest examination of

tested in the laboratory.

In Pattern 3, two of the Partner pairs met the three conditions for success previously stated. In pair C_1-C_2, the same conditions occurred as in the faulty pair of Pattern 2. Only one mine fuze functioned, yet the detonator in that mine did not fire. This pair, however is more easily explained: a connecting plug in the chassis was found disconnected. This would mean the circuit was disconnected from the

70

SECRET

battery and no energy was available to fire the detonator. Although the plug could have come loose after the test when the mine was dug up, it is believed that it occurred before the test.

Although the two failures of the circuitry encountered in the test might be explainable, they nevertheless point out the vulnerability of a complicated system. Furthermore, the problem of one pressure plate depressing when the other does not still exists and can be overcome only be design change.

A.4 CONCLUSIONS AND RECOMMENDATIONS

A.4.1 High Hat. High Hat is a workable design offering significantly better resistance to clearance than the unprotected mine. This performance can be improved by further reducing the area of the hat.

High Hat also offers the advantage of requiring no modification of the mine fuze. It is recommended that work on this design be continued.

A.4.2 Partner. The Partner system has the disadvantages of being complicated, of requiring modification of the mine fuze, and of offering little protection in the range of pressures where 10 to 90 percent of unprotected mines could be expected to function. However, the system does work well at higher pressures.

Although the disadvantages could be overcome by redesign, newer systems under development offer more promise. It is recommended that the design be reviewed to determine whether further work on it should be continued.

71

SECRET

Appendix B

VULNERABILITY of CERTAIN ANTITANK-INFLUENCE-MINE FUZES to NUCLEAR DETONATIONS

The purpose of this experiment was to determine the vulnerability of three antitank-influence-mine fuzes, designed at Diamond Ordnance Fuze Laboratories (DOFL), to a nearby nuclear detonation.

The three fuzes available for this purpose were the T 1217E2, the T 1224E1, and the T 1235. The T 1217E2 is a prototype; the T 1224E1 has been released for production engineering; the T 1235 represents an experimental design. All three fuzes are a part of a family of influence fuzes for use with the T-29 mine.

B.1 BACKGROUND

The following were considered as possible factors that would affect the vulnerability of a fuze to a nuclear detonation: (1) direct physical damage, which would make the fuze or mine inoperative, such as breakage of the case, damage to components, uncovering or tilting of the round; (2) functioning of the fuze during the detonation by presence of its normal functioning influences, such as pressure, vibration of the ground, magnetic fields, gamma radiation; (3) abnormal operation of the fuze sensing devices, e.g., closure of the magnetic switch in the T 1224E1 by excessive shock; (4) improper functioning of protective devices incorporated in the fuze, e.g., the blast protective switch in the T 1217E2 or the T 1224E1; (5) temporary sterilization due to discharge of firing capacitors by ionization; and (6) temporary sterilization of the T 1235 fuze by induced radioactivity in either the soil or the NaI scintillation crystal in the fuze.

B.2 PROCEDURE

An experimental program that would determine the exact behavior of the fuzes involved could not be attempted during this operation, because none of the items had been made in any appreciable quantity and, therefore, were in short supply. The limited program was intended to provide guidance for future tests with larger quantities, to initiate work on protective devices or on modification (should such prove to be necessary), and to correlate fuze behavior with data gathered by Diamond Ordnance Fuze Laboratories.

The 30 fuzes available for this test were equipped with detonator simulators to indicate fuze operation without causing damage to the fuze. This made possible reuse of the fuze and postshot examination of its sensitivity. All but the T 1235 were mounted on inert-loaded T-29 mine cases from which all firing-train components had been removed. A battery-operated clock, to indicate the time at which each fuze functioned (if functioning occurred), was attached to the bottom of each unit.

B.3 DESCRIPTION OF FUZES

B.3.1 T 1217E2 Fuze. This fuze used tank-track pressure as its influence but differed from a conventional pressure fuze in that simultaneous pressure of both tank treads was required to insure mine functioning underneath the belly of a tank. The sensing element was a pair of 8-foot rubber tubes, $\frac{1}{8}$ inch in outside diameter, one extending to either side of the fuze. The tubes were buried with from 1 to 4 inches of soil cover. The squeezing of a short length of each hose, as occurs on the overhead passage of a tank from both of its tracks, closed an electrical switch in the fuze. Both switches must close at nearly the same time to complete the firing circuit from a charged capacitor to an electrical detonator. In this way, firing of the mine underneath the tank and somewhere between both tracks is assured.

The fuze is kept inoperative initially for about $\frac{1}{2}$ hour by an arming delay clock to provide a safe period for burial of the mine, camouflaging, and departure of personnel from the area.

To prevent the fuze from firing on shock from the explosion of nearby mines or mine-clearance devices, a blast switch is built into the electrical circuit. When subjected to a downward acceleration of 1 to 2 g, the switch closes and sterilizes the fuze for about 10 seconds. Figure B.1 shows the T 1217E2 fuze in place on the T-29 mine, and Figure B.2 shows the mine and fuze in place, ready for covering.

B.3.2 T 1224E1 Fuze. This was a dual-influence fuze requiring both a vibration and a magnetic signal of proper characteristics as provided by a target tank crossing the mine to initiate the detonator. These signals could occur simultaneously or in close sequence, and their characteristics were determined by extensive studies on a large number of tanks. As in

72

SECRET
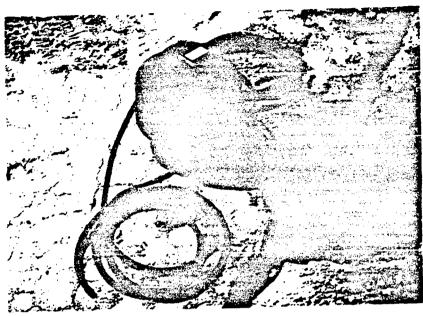
Figure B.1 T 1217E2 fuze with T-29 mine ready for placement.
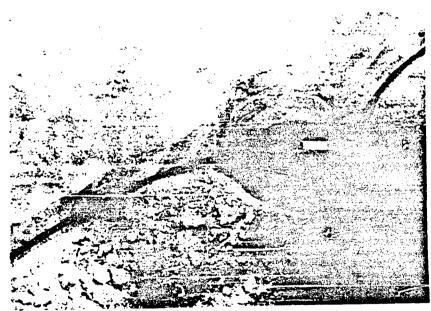
Figure B.2 T 1217E2 fuze with T-29 mine in place before burial.

73

SECRET

the T 1217E2 fuze, arming delay was accomplished by a spring-wound clock.

The magnetic sensing element was a moving magnet system, and protection against its closure by severe shock excitation was provided by the same blast switch as in the T 1217E2 fuze.

The optimum standoff distance of the mine to the target tank determines the burial depth of approximately 2 to 5 inches below grade. Figures B.3 and B.4 show the mine-fuze combination. Figure B.3 shows, on the bottom of the mine, the aluminum case that houses the electrical clock described in Section B.2. This clock, which was used for field-instrumentation purposes, is not a normal part of the mine.

B.3.3 T 1235 Fuze.
This was an experimental dual-influence fuze that required both a vibration signal and a gamma-ray signal originating from an externally buried source and backscattered from the target tank. Previous analyses and tests showed the fuze system capable of discriminating between heavy military vehicles, such as tanks, and lighter vehicles, such as jeeps and trucks.

It is difficult to countermeasure this fuze by normal methods; however, calculation has shown that a nuclear detonation could temporarily neutralize the system by blinding it with fallout or induced radioactivity in either the soil or the scintillation crystal used in the fuze detection system. The purpose of this experiment was to verify the supposition that the initial gamma radiation from the explosion would blind the fuze before the arrival of the shock wave (and therefore before arrival of the vibration influence) and to determine whether the system could be permanently damaged by high gamma and neutron fluxes. For this purpose the external gamma source, which would normally be buried with the fuze, was not needed and was omitted.

Since the fuze is still in the experimental design state, no photographs of the fuze are presented in this report.

B.3.4 Power Supplies.
All the fuzes used electrical detonators and required internal power supplies. General Electric T8 solid-state batteries were used in each fuze in conjunction with Mylar-insulated capacitors.

B.4 INSTRUMENTATION

B.4.1 Explosive Switch.
Each of the fuzes was equipped with a DOFL T-23 explosive switch. The electrical function and input characteristics of this device closely matched those of the T-76 electrical detonator and the T-29 mines.

The T-23 switch contained two pairs of contacts, one normally open and one normally closed. On fuze functioning when the switch is fired, the open contacts close and the closed contacts open. For this test, the normally open contacts were brought out from the buried mine to the surface of the ground by means of a shielded cable (Figure B.4). An ohmmeter was used at the time of recovery to determine whether functioning had occurred without disturbing the fuze. Stimulation of the fuze-sensing elements by simulation of the usual influence was performed if no functioning had occurred during the shot. The fuze's response to the proper influence was then observed on the ohmmeter. The normally closed pair of contacts were connected so as to stop the electrical timing clock (described below) at the time the switch fired.

B.4.2 Timing Clock.
This auxiliary timing device was used for the test to enable personnel to determine the time of fuze functioning relative to the time the fuze had been armed. It was attached beneath the fuze as shown in Figure B.3. The opened clock is shown in Figure B.5. Power supplied by a mercury battery gave the clock a running time from 7 to 14 days. Accuracy of the readings was approximately 15 minutes.

B.4.3 Charged Capacitors.
Included in the 1217E2 fuzes were several charged capacitors of the same type used in the fuzes. It was intended to observe their voltage decay after recovery and compare this with their ordinary decay rate. The desired information was the ability of a nuclear detonation to increase the decay rate and, thus, temporarily sterilize the fuze. It should be noted that, if this were to occur, the recharging rate with the very-high-impedance solid-state batteries would be low.

B.4.4 Location of Fuzes.
Three areas, each about 30 by 33 feet, were utilized near the eastern edge of the mine field at mean radial distance of 1,250, 2,730, and 5,320 feet, respectively, from ground zero. These distances were chosen to correspond to estimated overpressures of 60, 10, and 5 psi. Figure B.6 shows the location of these three areas, and Figures B.7, B.8, and B.9 show the distribution of fuzes within each of these areas. Of the six T 1217E2 fuzes, two were placed in each area; six of the twelve T 1224E1 fuzes were placed in the 1,250-foot area, and three each in the other two areas; the twelve T 1235 fuzes were evenly distributed, four in each area. The T-20 mine case, but not necessarily the explosive contents, is essential for proper operation of the T 1224E1 fuze, since the steel from which the case is fabricated is taken into consideration in adjusting the magnetic sensitivity of the fuze. The T 1217E2 and the T 1235 did not require mine cases for their proper performance; however, since 18 such cases were available for the test, they were used with the T 1224E1 and T1217E2 fuzes.

Mine positions were located and holes to the desired depths were provided by personnel of ERDL.

74
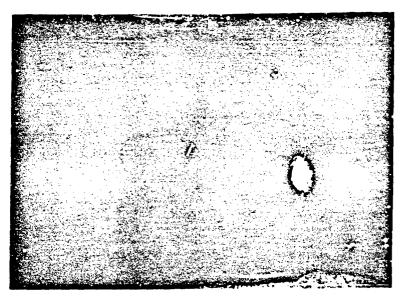
Figure B.3 The T 1224E1 fuze with T-29 mine and indicator clock.
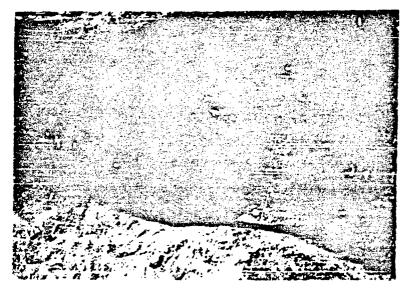
Figure B.4 The T 1224E1 fuze with T-29 mine in place before burial.

SECRET

Figure B.5 Seven-day electric clock.
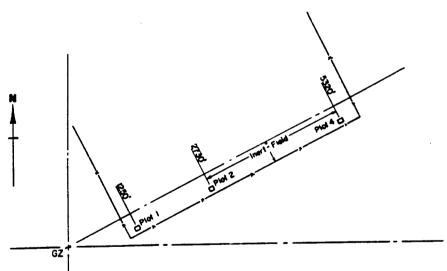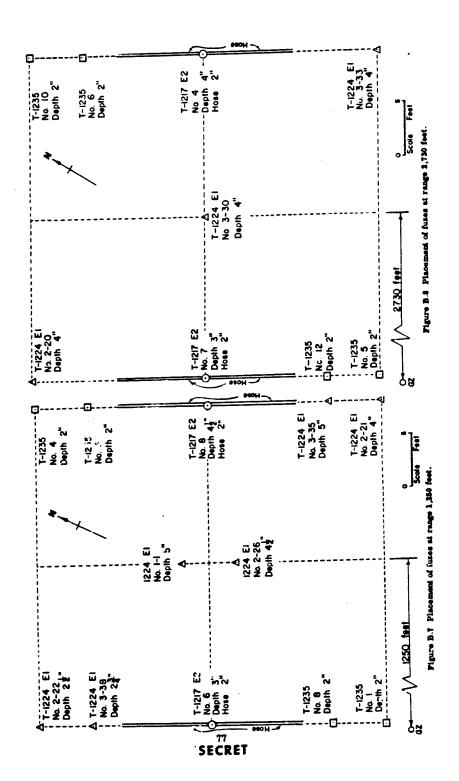
Figure B.6 Area location from ground zero.

SECRET

Figure B.8 Placement of fuses at range 2,730 feet.

Figure B.7 Placement of fuses at range 1,350 feet.

Some thought was   he unique soil conditions
prevailing in the *   .2 Dry Lake area. Before
disturbance, this a   .us the consistency of adobe
brick, while the d'r. dug from a hole has the texture
of talcum powder. Water was u..ed to stabilize the
soil backfilled around and over the mines. Some of

at 0630 hours on 24 June, so that a minimum of 3 days
had elapsed after planting for the fuzes to stabilize
in the ambient conditions. This r..riod was more
than sufficient for proper operation, even under the
severe soil conditions. Recovery of all units was
completed on the morning of 28 June. The same per-
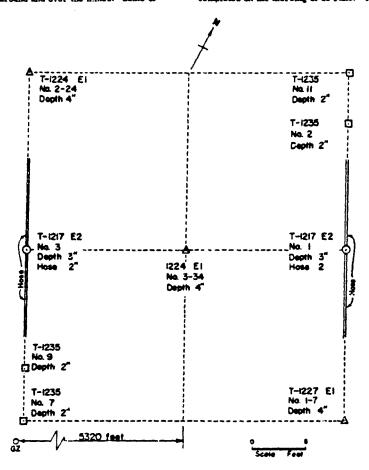
Figure B.9 Placement of fuzes at range 5,320 feet.

the soil was mixed with water to make a mortar, and
some was wetted by puddling in the hole. Each unit
was wrapped in a square of plastic sheeting before
burial to reduce contamination of the units by the soil;
however, it was later found that water and mud had
reached many of the fuzes.

B.3 RESULTS

Planting of the fuzes was performed during the
period from 16 to 21 June. Shot Priscilla was fired

sonnel who planted the mines performed the recovery
under full radex conditions in about an hour. This
included the checking of each fuze for functioning and
sensitivity. At the close-in area (1,250 feet to ground
zero), the radiation intensity was 125 mr/hr at recov-
ery time, the middle area had an intensity of 7 mr/hr,
and the farthest-out group had less than 1 mr/hr.

None of the fuzes or mines showed any physical
damage; however, a few of the timing-clock cases
were slightly dented. Brass stakes protruding about
3 inches above the ground had been used as markers.

78

These stakes, which were $\frac{1}{2}$ inch in diameter, were all in place but bent about 30 degrees from the vertical. In the middle area, about 20 feet of barbed wire (a part of the original mine field fence) was found covering one of the fuzes.

B.5.1 T1217E2 Fuzes.
None of the six units had functioned. When the hoses were squeezed at the time of recovery to simulate a normal signal, all of these fuzes operated. Simulation of the signal in this case was done manually, since no tanks were available. An examination of the soil covering the hoses indicated the results would have been unaltered if a tracked vehicle had been used.

B.5.2 T1224E1 Fuzes.
Two of the fuzes in the close-in area (1,250 feet from ground zero) functioned at the time of the shot. None of the remaining ten fuzes fired, including four fuzes at the same distance from ground zero as the two that did function. All unfired fuzes functioned properly when stimulated by vibration and magnetic signals before disarming and removal.

Blast switches were removed from the two fuzes that functioned in Shot Priscilla and replaced with special protective switches which were sensitive to prompt gamma radiation. These two reinstrumented fuzes and two other unmodified fuzes as controls were exposed about 800 feet from ground zero in Shot Hood. None of these four fuzes were functioned at the time of the shot. Except for one control failure, all functioned properly on postshot stimulation prior to disarming and removal.

B.5.3 T1235 Fuzes.
None of the twelve fuzes were fired by the nuclear detonation; however, one unit in the area closest to ground zero had apparently fired at H minus 25 hours. These results were not considered conclusive, since six of the twelve fuzes had fired on vibration signals alone at the time of emplacement. Later examination revealed the reason for this as being an increase in the fuze battery voltage attributable to the low relative humidity of the Nevada climate. This fault has been corrected by a modification in the power supply and vibration alerting circuit.

Because of the neutron-induced gamma activity in the scintillation crystal detectors and in fuze components, it was not possible to fire any of the fuzes at recovery time by means of simulated vibration and gamma-ray signals. This confirmed pretest calculations on the magnitude of the induced activity.

Although these fuzes were experimental models, constructed without regard to ruggedness, permanent damage was almost negligible. After a cooling-off period of a few weeks, normal fuze operation was restored.

The present design of the fuze is such that fuzes are expected to recover from the blinding effect of neutron-induced gamma activity in 24 to 48 hours after the fuzes have been exposed to 10^{12} neutrons/cm^2.

B.5.4 Charged Capacitors.
Laboratory examination revealed no difference between the ordinary and postshot decay rates of charged capacitors.

B.5.5 Gas Diodes.
Miniature gas diodes (XDIC, XD4C), exposed in several shots, showed promise as nuclear desensitizing switches for fuze use. For a 20 kt air-burst device, diodes biased at 95 percent of their normal breakdown voltage can be triggered reliably at ranges as great as 1 mile by instantaneous gamma radiation.

B.6 CONCLUSIONS AND RECOMMENDATIONS

No firm conclusions can be drawn from the meager data at this point. It appears that outlook for proofing of the T1217E2 and T1224E1 fuzes against clearing attempts by nuclear detonation is good. Several devices under development should reduce clearance percentages to low figures. The most important need is to establish a larger background of data from a better statistical sample. For this purpose the preliminary data gathered in this operation will be most helpful.

SECRET

Appendix C

GROUND CONTAMINATION PATTERNS PRODUCED
by E-5 CHEMICAL LAND MINES

The objective of this test was to determine qualitatively the ground contamination pattern produced by E-5 chemical land mines detonated by a nuclear explosion.

The E-5 chemical land mine is a standard M-15 mine except that it contains about 10 pounds of chemical-warfare agent and only about 0.7 pound of explosive material instead of a full explosive charge. Thus, the E-5 chemical land mine is designed so as to contain just enough explosive to scatter the liquid filling and contaminate an area adjacent to the mine when the mine is activated by means of normal M-15 mine-fusing techniques. For this particular test, a chemical warfare agent simulant, Bis 2-ethyl hexyl hydrogen phosphite, was used.

Five E-5 chemical land mines filled with the simulant agent were positioned 15 yards apart in a section of a Project 6.1 mine field where 8 to 9 psi overpressure was expected. Because this pressure is less than that required to guarantee detonation of the M-15, the mines were connected to a 2-psi sensitive detonation system. Points at which samples would be taken after the test were marked by 2-foot metal stakes driven into the ground so that 4 to 7 inches protruded.

Following detonation of the mine, samples were taken at these grid points by scraping the soil from an area 6 inches by 6 inches to a depth of about $\frac{1}{4}$ inch and collecting this dirt in glass jars. The samples were returned to the Army Chemical Center and analyzed for dyed Bis content. The results are reported as milligrams of chemical simulant per square meter of area. The sampling grid extended 75 yards downwind and 20 yards upwind. The distance between sampling points was 5 yards in the region near the mine and was gradually increased at greater downwind distances.

Prior to Shot Priscilla, one chemical land mine was detonated in order to determine the contamination pattern produced without influence from shot conditions. In this test, which was conducted in a small area adjacent to where five mines were tested, samples of the soil in the area contaminated were collected from grid points at intervals of 5 yards out to distances of 25 yards from the mine. This test served to supply data for a normal pattern on the terrain in Frenchman Flat.

The area of contamination from the chemical land mines is shown in Figure C.1. The contaminated area from the detonation of a single mine is also

shown. It will be noted that only two of the five mines were detonated by the blast wave from the shot. While collecting samples after the nuclear detonation, it was observed that the ground in parts of the grid patterns had been distributed and/or covered by dirt during the period from blast to sample collection.
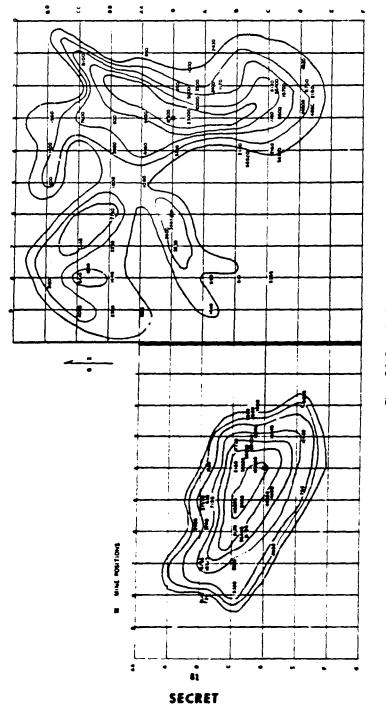
The test of the five mines during Shot Priscilla was not as successful as had been hoped because only two of the five mines were detonated. The patterns of the ground contamination from the two (blast-detonated) mines are dissimilar to the single munition; this difference also appears in other tests with the same munition conducted at Army Chemical Center. One of the blast-detonated mines had 33 times the quantity of agent normally found on the crater lip and essentially no contamination on the ground in the vicinity near the crater.

The difference between ground contamination patterns of the separate tests or between the two blast-detonated mines may be caused by reasons other than the method of detonation. These may be: (1) low-order burst of the one blast-detonated mine which had high crater-lip contamination, or (2) loss of contamination from the blast-detonated mines due to the surface being removed, disturbed and/or covered by blowing dirt during the period from burst to sample collection. Thus, it is difficult to compare the contamination patterns of the blast-detonated mines with that from normal detonation of a mine. However, the data indicate a difference in the distribution of ground contamination with the two different methods of detonation. These differences are not considered as conclusive evidence because of the limited number of tests, the conditions to which the area was exposed before the samples were collected, and the normal possibilities of low-order detonations.

Sufficient data were collected to demonstrate conclusively that, (1) residual toxic contamination will result when chemical mine fields are functioned by nuclear detonations, and (2) that a difference in contamination pattern can be expected when the E-5 chemical land mine is detonated by the blast from a nuclear detonation, over that pattern produced by detonation of the mine's pressure-sensitive fuse.

It is recommended that tests be conducted to obtain additional data concerning the area which might be contaminated if a nuclear weapon were used so as to detonate chemical land mines.

84

SECRET

Figure C.1 Contamination patterns.

Appendix D
TEST of BRITISH TYPE MINES for the UNITED KINGDOM

The objective of this test was to subject four types of British mines, the Mark VII, Mark 5, Light Metallic antitank mines, and the Elsie antipersonnel mine (Figures 2.16, D.1, D.2, D.3), to the blast from a nuclear detonation. It was particularly important to supplement existing British data on the reaction of these mines to atomic air blast and to check the correlation of British and United States records on the behavior of these mines.

D.1 BACKGROUND

The British have tested the Mark VII antitank mine on several occasions. This mine uses a Mark 5 fuze, which requires a double impulse to actuate the mine. No mines received both impulses at any of the trials. In some of the tests, the first impulse was applied in overpressure ranges between 32 and 250 psi. The results at pressures less than 32 psi did not obey any recognizable pattern.

The British tests of the Light Metallic antitank mine at depths of cover varying from 2 to 4 inches resulted in only about 3 percent firing at overpressures less than or equal to 30 psi. At higher pressures and comparable depths of burial, all mines were actuated. (These results do not agree with quoted United States figures on this mine).

Although the design of the spider-type pressure plate found on the Mark 5 antitank mine had not been tested under nuclear blast loading, it was believed that, because of the low resistance of the spider plate, the mine would require a greater force for actuation than mines with a solid pressure plate.

When subjected to British tests, there was no actuation of the Elsie antipersonnel mines at 30 psi overpressure and lower; for higher pressures, 50 percent or more fired. At overpressures greater than 25 psi, all mines were dislodged from their original placement position.

United States Army Engineer Research and Development Laboratories (ERDL), Fort Belvoir, Virginia, performed static actuation tests on the Light Metallic and Mark 5 antitank mines and the Elsie antipersonnel mine. (Tests were not performed on the Mark VII mine, since data on static-actuation pressures was already available from the work of the mine study reported in Reference 4.) Results of the tests are shown in Table D.1.

D.2 PROCEDURE

Because of the limited amount of time to arrange for shot participation, and problems of transportation of live explosives, all mines were inert-filled. The criteria for the method and ranges of placement, as well as depth of cover, were the desires and proposals of the British authorities. Since no analysis of results was required of the United States personnel conducting the test, a thorough investigation was not made of the reasons for the placement proposals. British suggestions were adhered to as closely as possible, i.e., attempts were made to place mines at pressure ranges used in the main project.

Positions for the British fields are noted in Figure 2.17 in the main body of the report. Table D.2 shows the ranges from ground zero, the suggested placement pressures, the predicted pressures for actual placement, the number of mines placed in each field, and the depth of cover over the mines. The holes for the antitank mines were dug with an earth auger; the diameter of the bit was adjusted to fit the needs of the mine. The holes for the Elsie mines were dug with a pocket knife so that the diameter was the same as that of the body of the mine.

From the results of the previous British tests on the Elsie mine, it was decided that those placed at estimated overpressures of 21, 14, and 5 psi would not be dislodged from their holes. Precautions were taken to hold the Elsie's in position at the estimated overpressure of 30 psi by a thin wire tied to the body of the mine and fastened to a pipe driven into the ground (Figure D.4).

The elsie's were fabricated from two different types of plastic, one black in color and the other white. An equal number of each type were planted at each range.

D.3 RECOVERY

Test instructions specified that cursory examination be made of the fuzes to determine possible actuation. In addition, it was requested that observations be made to determine (1) exposure or lifting of the mines by blast, and (2) external damage to the mine body by blast or by thermal radiation. In addition, the Elsie's were also examined for disturbance from position and burning of the camouflage covering the pressure plate. After this preliminary examination,

82

SECRET
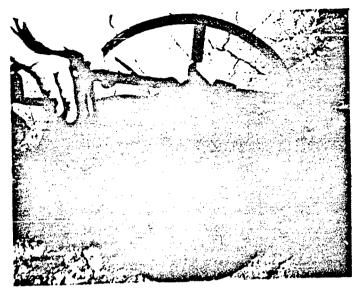
Figure D.1 British, Mark 5 antitank mine.
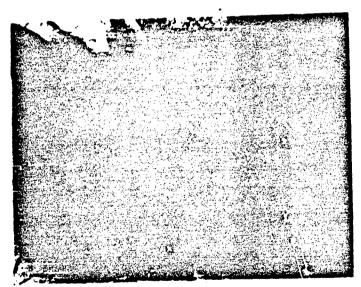
Figure D.2 British, light metallic antitank mine.
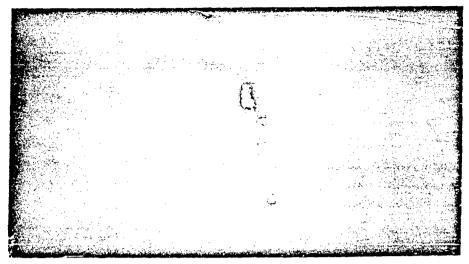
Figure D.3 British, Elsie, antipersonnel mine.
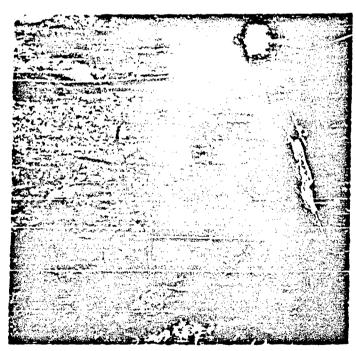
Figure D.4 Tiedown of Elsie, antipersonnel mine.

84

SECRET

TABLE D.1 RESULTS OF STATIC-DEFLECTION TESTS

Mine Type	Average Static Actuation Pressure (Average of three samples)	Pressure Plate Area
	psi	in²
Light Metallic	16.1	28.3
Mark 5	83.7	4.0
Elsie	11.1	0.79

TABLE D.2 MINE PLACEMENT

The space between mines was three feet

Type	Suggested Placement Pressure	Range	Predicted Pressure	Cover	Quantity Per Range
	psi		psi	inch	
Mark VII	150	920	150	2	7
	100	1,040	100	2	7
	60	1,250	60	2	7
Mark 5	150	920	150	0	7
	100	1,040	100	0	7
	60	1,250	60	0	7
Light Metalic	45	1,500	40	2	7
	30	1,720	30	2	7
	15	2,290	15	2	7
Elsie	45	1,720	30	0	4
	30	1,990	21	0	4
	20	2,290	15	0	4
	10	5,320	5	0	4
	5				

TABLE D.3 OVERPRESSURES

The overpressures at 920 and 1,040 feet are interpolated from Figure G.3.

Range	Predicted Overpressure	Actual Overpressure
feet	psi	psi
920	150	160 to 200
1,040	100	115 to 140
1,250	60	76
1,370	50	60.5
1,500	40	43.5
1,720	30	28.9
1,990	21	20.6
2,290	15	16
5,320	5	5.4

85

TABLE D.4 ANTITANK RESULTS

Mark VII, 920 feet	□	□	□*	□	□	□	□
Mark VII, 1,040 feet	□	□	□*	□	□	□	□
Mark VII, 1,250 feet	□	□	□	□	□	□	□
Mark 5, 920 feet	□	□	○†	□	○	□	○
Mark 5, 1,040 feet	○	○	○	○	○	○	○
Mark 5, 1,250 feet	○	○	○	○	○	○	○
Light Metallic, 1,500 feet	○	□	□	□	□	)	□
Light Metallic, 1,720 feet	□	□	○	□	□	□	○
Light Metallic, 2,290 feet	○	○	□‡§	○	○§	○§	○§

* Fuze jammed.
† Pin partially sheared.
‡ Run over by vehicle.
§ Six inches of cover.
○ ... not actuated.
□ ...

TABLE D.5 ELSIE RESULTS

Range	Plastic	Fuze Actuated	Remarks
feet	color		
1,720	White	Yes	Mine found about 400 feet back from original position. Camouflage nearly burned or blown off. Upper front portion of body "wrinkled" by thermal. Charge container slightly burned at front. Front $\frac{1}{3}$ of body collar broken off at point where wire originally attached.
	Black	Unknown	Only top portion of mine body found. Top portion of body found 400 feet back from original position. Charge container found 550 feet back from original position. Mine broken in half under body collar. Camouflage burned off.
	White	Yes	Camouflage nearly burned off. Front part of body "wrinkled." Top surface of body burned and blackened. Charge container slightly burned at front.
	Black	Unknown	Mine not found.
1,990	White	Yes	Camouflage burned off. Upper front portion and top of body slightly burned and wrinkled.
	Black	Unknown	Mine not found.
	White	Unknown	Mine not found.
	Black	Unknown	Mine not found.
...	White	No	Camouflage nearly burned or blown off. Upper front portion of body wrinkled. Otherwise, mine in good condition.
	Black	No	Camouflage nearly burned or blown off. Otherwise, mine in good condition.
	White	No	Camouflage nearly burned or blown off. Otherwise, mine in good condition.
	Black	Yes	Camouflage nearly burned or blown off. Otherwise, mine in good condition.
5,230	White	Yes	Camouflage nearly burned or blown off. Top surface of charge container burned and melted. Top surface of body slightly melted in front and back.
	Black	No	Camouflage burned or blown off. Otherwise mine in good condition.
	White	Yes	Camouflage burned or blown off. Otherwise mine in good condition.
	Black	No	Camouflage burned or blown off. Otherwise mine in good condition.

the mines were to be returned to the United Kingdom for detailed internal examination and statistical analysis.

D.4 RESULTS AND DISCUSSION

Results of the postshot investigation of the British mines in this project are summarized in Tables D.4 and D.5. Actual and predicted peak overpressures are compared in Table D.3.

The combined results of the layout for the United Kingdom investigation and the layout for the main Project 6.1 for the Mark VII mine agree well with the pretest British data on the mine. The lower limit (where insufficient compression for arming or activation can be expected) can be estimated from the main field data of Project 6.1 to be about 20 psi overpressure. It was also observed that, for pressures of 60 psi or more, all mines will receive the first impulse but no mines will be actuated, i.e, none of the mines receive the double impulse.

The spider-plate design for the pressure plate of the Mark 5 mine seems to be an effective device for withstanding large overpressures as was expected. At the closest range of 920 feet from ground zero, four out of seven of the mine fuzes functioned, indicating that their live prototypes would have detonated. At the 1,040-foot range, where the overpressure was at least 115 psi, none of the fuzes functioned. The same was true at the 1,250-foot range. Two values are therefore available from the test data from which the statistical analyst may be able to plot a probability-of-actuation curve for given overpressures.

Not as much useful data was obtained for the Light Metallic Mine as had been anticipated. At overpres-

sures of 43.6 and 28.9 psi, five of the seven mine fuzes functioned. These do not coincide with existing British data on the actuation pressures for this mine. Caution must be taken in comparing the data taken from the mines placed at the 2,290-foot range, owing to experimental errors: (1) five of the mines were buried with 6 inches of cover, instead of the required 2 inches; and (2) a vehicle was driven over one mine before recovery was made.

The following observations were made on the Elsie antipersonnel mine:

1. The cloth camouflage covering the pressure plate was completely burned or blown off in almost all cases.

2. The body of at least one mine at each range studied was severely affected by thermal radiation, resulting in wrinkling and charring. In some cases, the fuzes for these burned mines did not actuate. Suprisingly, the black plastic mines withstood thermal effects better than the white mines in every instance.

3. Six of the mines were thrown out of their holes by the drag pressure; two were found, of which one had been actuated while the other had been shattered. A thorough search of the area disclosed no evidence of the remaining four antipersonnel mines These mines were completely inert (contained no explosives) and therefore the loss would in no way prove dangerous to anyone should the mines be uncovered at a later time.

4. Some fuzes were actuated at each range without following any recognizable pattern for proportion actuated. This portion of the study was hampered by the fact that not all the mines were recovered.

5. The blast severely cracked the mine casing at the highest range of pressure studies.

Appendix E
SYMPATHETIC DETONATION ANALYSIS

E.1 PROBABILITIES OF DIFFERENT RANDOM PATTERNS IN MINE DETONATION

The geometric pattern of mine actuation in the live minefield may give an indication of whether sympathetic detonation was present. Intuitively, if each mine that actuated in a live mine field were adjacent to another actuated mine, the likelihood of sympathetic detonation would be increased.

Each geometric actuation pattern that was encountered in the live mine field was either due to a random geometric distribution or a nonrandom distribution. It was assumed that nonrandom distributions were due to the effect of sympathetic detonation. One mine detonating could result in another mine detonating only if the distances between mines were small. It was assumed that the radius of influence for one mine to cause detonation of another mine was the maximum distance between adjacent mines, or 21 feet. Therefore, the detonation of at least two adjacent mines was the criterion for the possibility of sympathetic detonation.

When the probability of the random occurrence of the actuation pattern encountered in each mine field is known, one may determine the likelihood of sympathetic detonation. If the random probability was small for the geometric actuation pattern encountered in the mine field, then the probability was high that sympathetic detonation had contributed to the number of actuations. (This would exclude actuation patterns where, by definition, sympathetic detonation was impossible.)

The probability of random actuation patterns was determined for 1 to 10 mine, detonating respectively (Table E.1). It was required to know the probability of a random actuation pattern occurring that was at least as favorable to sympathetic detonation as the pattern of the test. For this reason the probabilities are listed in order, with the most favorable pattern for sympathetic detonation listed first. With a given number of mines actuating, the pattern most favorable to sympathetic detonation was the pattern with the greatest number of arrangements where two adjacent mines actuated.

No simple method was found for determination of the probability of the random occurrence of a given pattern. All combinations were enumerated and combinations with a specific pattern were divided by the total combinations to give the probability of the

particular pattern occurring. Each specific pattern was further broken down to arrive at the total number of arrangements under which sympathetic detonation could happen. This was to allow ranking in order of favorability to sympathetic detonation.

The nomenclature used for the random probability will be explained by an example. The expression $P_3(1, 2)$ means the probability of three mines actuating when two of the mines are adjacent (less than 21 feet between mines) and the third mine is separated from the other two by at least one mine that did not detonate.

E.2 PROBABILITIES OF RANDOM VARIATION OF TEST POINTS FROM TRUE CUMULATIVE PROBABILITY CURVE

Each sample (pattern) can be considered as composed of independent trials where the true probability of the mine actuating in a single trial is given by the cumulative normal probability distribution. From the theory of probability, the equation for independent trials is given by the terms in the binomial expansion.

$$(q+p)^n = \sum_{r=0}^{n} C_r^n q^{n-r} p^r$$

Where: $C_r^n = \dfrac{n!}{r!(n-r)!}$

p = probability that a single mine will actuate

q = probability that a single mine will not actuate

n = number of trials

r = number of mine actuations

$C_r^n q^{n-r} p^r$ = probability of exactly r mines actuating in n trials.

Since the likelihood of sympathetic detonation increases as the percentage of mines that actuate increases, it is easy to rank random probabilities in order of favorability to sympathetic detonation. The higher the test percentage, the more favorable are conditions for sympathetic detonation.

The probability that a test value from the live mine field would be as great or greater due to random variation is given by the sum of all terms from r through n in the binomial expansion. The value of

92

p to use is determined from the cumulative probability curve at the inert mine-field overpressure. It is assumed that for random variation in the mines the same overpressure would also apply in the live mine-field.

As an example, the probability will be computed that a detonation test value of the M/47-I mine could

in the live mine field, $n = 10$, the appropriate binomial expansion is:

$$(q+p)^{10} = \sum_{r=0}^{10} C_r^{10} q^{10-r} p^r = 1$$

$$= q^{10} + 10q^9p + 45q^8p^2 + 120q^7p^3 + 210q^6p^4$$

TABLE E.1 PROBABILITIES OF RANDOM DETONATION PATTERNS

I. Two Mines Detonating			**VI. Continued**	
$P_2(2)$	$= 14/25$		$P_7(2,5)$	$= 16/120$
$P_2(1,1)$*	$= 31/45$		$P_7(1,2,4)$	$= 8/120$
			$P_7(2,2,3)$	$= 2/120$
II. Three Mines Detonating			$P_7(3,4)$	$= 20/120$
$P_3(3)$	$= 20/120$		$P_7(1,2,2,2)$	$= 0$
$P_3(1,2)$	$= 68/120$		$P_7(1,1,2,3)$	$= 0$
$P_3(1,1,1)$*	$= 32/120$		$P_7(1,1,2,2)$	$= 0$
			$P_7(1,1,1,4)$	$= 0$
III. Four Mines Detonating			$P_7(1,1,1,1,3)$	$= 0$
$P_4(4)$	$= 28/210$		$P_7(1,1,1,1,1,2)$	$= 0$
$P_4(1,3)$	$= 72/210$		$P_7(1,1,1,1,1,1,1)$	$= 0$
$P_4(2,2)$	$= 35/210$			
$P_4(1,1,2)$	$= 66/210$		**VII. Eight Mines Detonating**	
$P_4(1,1,1,1)$	$= 0$		$P_8(8)$	$= 32/45$
			$P_8(3,5)$	$= 2/45$
IV. Five Mines Detonating			$P_8(1,7)$	$= 4/45$
$P_5(5)$	$= 40/252$		$P_8(4,4)$	$= 3/45$
$P_5(1,4)$	$= 64/252$		$P_8(2,6)$	$= 4/45$
$P_5(2,3)$	$= 64/252$		$P_8(2,3,3)$	$= 0$
$P_5(1,1,3)$	$= 38/252$		$P_8(2,2,4)$	$= 0$
$P_5(1,2,2)$	$= 34/252$		$P_8(1,3,4)$	$= 0$
$P_5(1,1,1,2)$	$= 12/252$		$P_8(1,2,5)$	$= 0$
$P_5(1,1,1,1,1)$	$= 0$		$P_8(2,2,2,2)$	$= 0$
			$P_8(2,3,3,3)$	$= 0$
V. Six Mines Detonating			$P_8(1,1,2,2,2)$	$= 0$
$P_6(6)$	$= 57/210$		$P_8(1,1,3,3)$	$= 0$
$P_6(2,4)$	$= 38/210$		$P_8(1,1,2,4)$	$= 0$
$P_6(1,5)$	$= 42/210$		$P_8(1,1,1,2,3)$	$= 0$
$P_6(2,2,2)$	$= 4/210$		$P_8(1,1,1,1,2,2)$	$= 0$
$P_6(1,1,4)$	$= 18/210$		$P_8(1,1,6)$	$= 0$
$P_6(1,2,3)$	$= 24/210$		$P_8(1,1,1,5)$	$= 0$
$P_6(3,3)$	$= 23/210$		$P_8(1,1,1,1,4)$	$= 0$
$P_6(1,1,2,2)$	$= 4/210$		$P_8(1,1,1,1,1,3)$	$= 0$
$P_6(1,1,1,3)$	$= 0$		$P_8(1,1,1,1,1,1,2)$	$= 0$
$P_6(1,1,1,1,2)$	$= 0$		$P_8(1,1,1,1,1,1,1,1)$	$= 0$
$P_6(1,1,1,1,1,1)$	$= 0$			
			VIII. Nine Mines Detonating	
VI. Seven Mines Detonating			$P_9(9)$	$= 1$
$P_7(7)$	$= 52/120$			
$P_7(1,6)$	$= 20/120$		**IX. Ten Mines Detonating**	
$P_7(1,1,5)$	$= 2/120$		$P_{10}(10)$	$= 1$

* With this pattern, sympathetic detonation is impossible.

have been as large or larger because of random variation. The test point chosen was the 26.7-percent actuation point at 11.6-psi static overpressure. From the cumulative probability curve, the predicted actuation at this pressure is 10 percent. This value is assumed to be the true probability, p, that a single mine will actuate at 11.6 psi. For the sample size

$$+ 252q^5p^5 + 210q^4p^6 + 120q^3p^7 + 45q^2p^8$$
$$+ 10qp^9 + p^{10}$$

Where: $p = 0.1$

$q = 0.9$

For the probability of one or more random mines

actuating, the terms of the binomial expansion must be added from $r = 1$ through $r = 10$. Therefore, the probability is:

$$\sum_{r=1}^{10} C_r^{10} q^{10-r} p^r = 1 - q^{10}$$

$$= 1 - (0.9)^{10} = 0.651$$

This means that if the probability of a single mine actuating at 11.5 psi is $p = 0.1$, then the probability of at least one mine (one or more) actuating in a sample size of 10 is 0.651.

The values of p were computed to an accuracy of two decimal places which was considered more than adequate for the reliability of the data.

Appendix F
SUMMARY of RAW DATA

This appendix presents raw data from the mine field clearance operation. Data from the inert mine fields are presented in Figures F.1 through F.13, while the live mine field data can be found in Figures F.14 through F.26. The meter readings and gaps from the pressure plate to the fuze for the UIM from the depth-of-burial study are given in Table F.1; the same UIM data from the study of the effect of load type upon the mine response is found in Table F.2.

Range, Feet	Overpressure, psi	Percent Actuation
2520	10.9	0

Range, Feet	Overpressure, psi	Percent Actuation
2730	8.7	0

Range, Feet	Overpressure, psi	Percent Actuation
3250	8.7	0

O = Mine Location   ● = Activated Mine

Figure F.1 Results in inert mine field, M-15

Figure F.2 Results in inert mine field, N-19.

SECRET

Figure F-4 Results in inert mine fields, M/47-1I.

Figure F-3 Results in inert mine field, M/47-I.

Figure F.6 Results in inert mine fields, CC-48.

Figure F.5 Results in inert mine fields, M/52.

94

SECRET

Figure F-7 Results in inert mine fields, CS-42/3.

Figure F-8 Results in inert mine fields, SACI.

Figure F.9 Results in inert mine fields, TMD-B.

Figure F.10 Results in inert mine fields, TM-41.

SECRET

Figure F.12 Results in inert mine fields, French 1951.
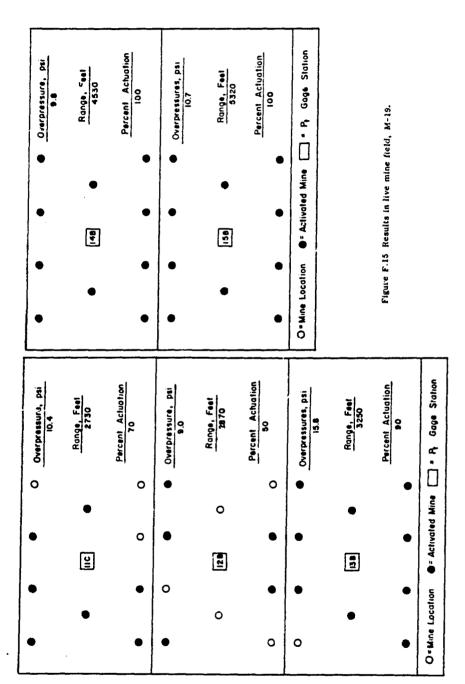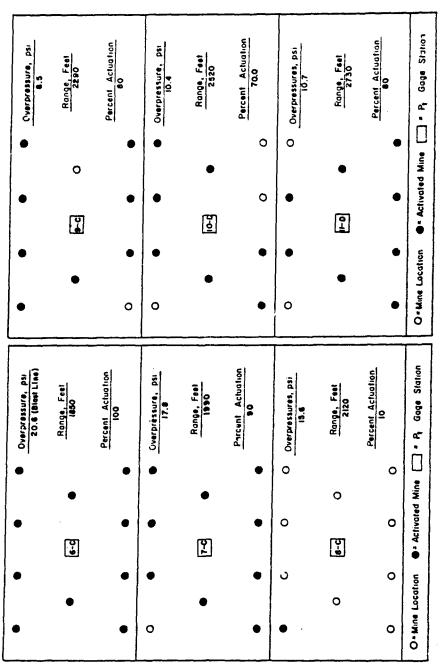
Figure F.11 Results in inert mine fields, FRB-ND-49.

Figure F-13 — Results in inert mine fields, Mark VII.

	Range, Feet	Overpressure, psi	Percent Actuation
Panel 1	1720	26.9	3.3
Panel 2	1850	20.6	3.3
Panel 3	1990	18	0

O = Mine Location   ● = Activated Mine

Figure F-13   Results in inert mine fields, Mark VII.

Figure F-14 — Results in live mine field, M-15.

	Overpressure, psi	Range, Feet	Percent Actuation
10B	11.1	2520	0
11B	9.1	2730	0
13B	9.7	3250	0

O = Mine Location   ● = Activated Mine   □ = P₁ Gage Station

Figure F-14   Results in live mine field, M-15.

98

Figure F.15 Results in live mine field, M-19.

Overpressure, psi
8.5

Range, Feet
2290

Percent Actuation
80

8-C

Overpressure, psi
10.4

Range, Feet
2520

Percent Actuation
70.0

10-C

Overpressures, psi
10.7

Range, Feet
2730

Percent Actuation
60

1-D

O = Mine Location   ● = Activated Mine   □ = P_t Gage Station

Figure F.17 Results in live mine field, M/47-II.

Overpressure, psi
20.6 (Blast Line)

Range, Feet
1650

Percent Actuation
100

5-C

Overpressure, psi
17.8

Range, Feet
1990

Percent Actuation
90

7-C

Overpressures, psi
15.6

Range, Feet
2120

Percent Actuation
10

6-C

O = Mine Location   ● = Activated Mine   □ = P_t Gage Station

Figure F.16 Results in live mine fields, M/47-I.

100

SECRET

Figure F.19 Results in live mine fields, CC-48.

Figure F.18 Results in live mine fields, M/52.

5-C — Overpressure, psi 14.4 · Range, Feet 1720 · Percent Actuation 30

7-F — Overpressure, psi 26.9 · Range, Feet 1990 · Percent Actuator 10

9-G — Overpressures, psi 14.7 · Range, Feet 2290 · Percent Actuator 0

O = Mine Location   ● = Activated Mine   □ = P_t Gage Station

Figure F.21 Results in live mine fields, SACI.

4-B — Overpressure, psi 38.7 · Range, Feet 1600 · Percent Actuation 90

6-F — Overpressure, psi 15.4 · Range, Feet 1850 · Percent Actuation 70

8-F — Overpressures, psi 18.5 · Range, Feet 2120 · Percent Actuation 20

O = Mine Location   ● = Activated Mine   □ = P_t Gage Station

Figure F.20 Results in live mine fields, CS-42/3.

Figure F.23 Results in inert mine fields, TM-41.

Figure F.22 Results in live mine fields, TMD-B.

Figure F.25 Results in live mine fields, French 1951.

Panel 2-B: Overpressure, psi 53.7; Range, Feet 1370; Percent Actuation 80

Panel 3-B: Overpressure, psi 43.0; Range, Feet 1500; Percent Actuation 80

Panel 6-B: Overpressures, psi 12.9; Range, Feet 1850; Percent Actuation 40

O = Mine Location   ● = Activated Mine   □ = P_f Gage Station

Figure F.24 Results in live mine fields, PRB-ND-49

Panel 8-G: Overpressure, psi 18.2; Range, Feet 2120; Percent Actuation 100

Panel 9-B: Overpressure, psi 12.6; Range, Feet 2290; Percent Actuation 70

Panel 10-C: Overpressures, psi 9.4; Range, Feet 2520; Percent Actuation 0

O = Mine Location   ● = Activated Mine   □ = P_f Gage Station

104

Figure F 26 Results in live mine fields, Mark VII.

TABLE F.1 RESULTS OF DEPTH OF BURIAL UIM

		Depth of Burial												
		0 inch		3 inches		6 inches		9 inches		12 inches		15 inches		36 inches	
Range	Peak Overpressure	UTM Reading	Gap	UTM Reading	Gap	UTM Reading	Gap	UTM Reading	Gap	UTM Reading	Gap	UTM Reading	Gap	UTM Reading	Gap
feet	psi	mils	mils	mils	mils	mils	mils	mils	mils	mils	mils	mils	mils	mils	mils
1,250	76	165	64	168	70	168	60	168	34	172	57	158	62	58	58
		162	76	167	57	167	57	167	62	164	47	169	66	52	56
		166	72	167	68	166	53	172	62	173	50	170	60	50	63
		168	58	170	70	172	48	164	37	161	58	171	38	63	55
		173	67	168	64	169	64	174	40	172	72	174	67	44	55
		-	-	173	71	160	64	168	55	173	71	170	66	62	62
		190	55	133	54	171	59	171	61	171	54	160	66	38	67
		169	77	175	66	162	41	160	72	170	54	172	52	47	75
		172	67	162	75	175	58	166	67	167	62	166	57	57	75
		164	67	171	54	176	66	190	64	167	52	162	72	46	60
Average		169.9	67.9	168.5	65.2	168.6	57.4	171.0	56.0	169.4	58.6	168.1	60.5	52.3	63.5
1,270	60.5	174	58	161	58	162	61	167	58	162	69	152	56	40	41
		169	54	173	62	168	59	169	44	173	34	126	56	29	55
		171	51	162	52	167	51	156	56	166	44	160	50	43	67
		169	69	164	59	168	61	163	8.	163	60	139	32	33	49
		157	62	-	-	165	54	166	60	163	51	141	56	30	53
		172	96	160	50	163	60	163	56	167	51	146	58	25	66
		176	69	164	73	164	49	165	63	157	70	96	74	36	57
		-	-	165	34	173	46	161	59	160	56	138	73	23	43
		171	56	172	66	160	64	175	66	159	52	134	40	32	60
		165	66	161	45	170	51	165	62	172	63	142	56	34	64
Average		168.7	62.3	164.7	56.1	166.0	55.6	165.2	63.9	164.7	57.5	139.1	54.3	36.0	36.1
1,500	43.6	39	61	50	54	154	60	168	52	132	42	127	56	21	50
		44	61	109	64	157	64	154	68	164	47	132	56	21	58
		36	51	60	62	151	62	162	65	143	59	64	61	29	44
		60	41	121	56	167	47	175	74	143	56	96	58	21	60
		47	56	64	53	146	57	162	68	153	60	155	60	22	65
		47	55	99	60	158	59	154	57	125	54	146	40	28	53
		63	66	93	36	135	73	169	62	170	53	134	50	33	46
		47	49	108	60	145	56	167	59	144	46	96	54	25	60
		67	49	123	41	143	51	123	57	132	47	66	80	31	55
		49	54	86	66	165	55	162	63	120	56	53	57	29	53
Average		54.6	53.2	94.5	55.2	150.2	56.4	160.6	60.9	142.6	51.2	104.5	56.6	24.5	54.7
1,730	28.9	41	49	44	53	78	38	103	49	64	41	36	47	16	53
		48	58	53	62	70	43	119	49	77	59	30	44	30	49
		48	47	52	53	98	51	117	57	90	54	33	54	32	39
		50	58	47	63	80	56	61	45	53	58	36	53	14	65
		58	40	39	39	130	60	110	50	53	53	30	56	12	58
		75	62	36	52	135	43	103	44	59	58	32	53	17	45
		70	38	51	44	111	24	59	56	47	40	36	40	12	65
		57	58	54	41	75	36	90	38	78	46	25	61	18	44
		64	57	37	43	83	62	106	35	106	46	35	48	15	39
		49	60	40	46	87	51	59	56	57	52	39	56	3	59
Average		55.2	53.7	45.3	52.6	93.7	46.6	92.7	49.0	67.4	51.6	32.5	50.1	16.4	49.6
1,900	16.6	16	49	36	31	37	38	46	*	62	43	31	40	29	49
		31	40	36	47	37	47	53	44	38	38	33	46	18	39
		16	34	30	53	51	47	62	48	54	43	43	33	36	43
		10	52	26	54	44	48	53	41	42	38	30	49	12	8.
		12	34	31	26	31	56	53	58	51	38	36	47	21	46
		16	36	30	43	35	61	70	40	36	43	36	54	18	47
		22	39	32	44	49	37	70	62	55	49	35	43	31	50
		15	39	29	32	13	34	86	50	50	51	33	51	21	55
		11	45	33	35	53	51	54	43	65	37	45	38	18	49
		25	33	17	28	46	37	56	45	60	46	32	52	25	60
Average		17.4	40.1	29.4	39.3	40.0	45.6	61.8	48.0	53.0	42.5	34.4	45.2	21.9	48.3

106

SECRET

Range	Peak Overpressure	Depth of Burial												
		0 inch		3 inches		6 inches		9 inches		12 inches		18 inches		36 inches	
		UIM Reading	Gap	UIM Reading ‡	Gap	UIM Reading	Gap	UIM Reading ‡	Gap	UIM Reading ‡	Gap	UIM Reading ‡	Gap	UIM Reading ‡	Gap
feet	pei	mils	mils	mils	mils	mils	mils	mils	mils	mils	mils	mils	mils	mils	mils
2,290	10.4	12	60	32	32	44	67	55	53	29	62	21	57	2	44
		12	47	30	71	43	52	50	47	27	48	19	48	7	27
		2I	42	32	49	36	63	40	60	27	53	9	56	9	32
		11	49	28	60	35	46	42	46	21	46	8	49	12	50
		6	59	27	61	38	66	?1	51	18	50	25	36	1u	53
		5	!?	4?	52	33	54	32	47	26	43	8	55	10	39
		16	40	?6	??	37	4?	38	49	18	48	15	48	1	44
		12	48	28	58	40	?1	13	50	37	3?	26	56	7	48
		22	41	24	60	5?	35	4?	57	35	39	22	38	12	46
		116 ?	40	43	??	45	44	25	50	16	58	18	50	10	45
Average		13.0†	46.9†	31.5	56.1	40.3	52.5	39.9	51.0	25.4	48.6	17.1	49.3	8.0	42.8
2,730	8.7	−6	34	8	75	17	61	25	57	??	56	15	54	−4	49
		*	*	8	*2	15	48	1?	55		56	10	48	−19	33
		−6	61	15	55	1?	55	13	65	14	49	7	53	−11	42
		−??	25	??	50	11	53	17	67	15	56	5	58	−7	35
		−24	38	13	59	11	56	17	56	18	34	0	60	−24	39
		−16	25	11	62	6	53	16	55	12	53	3	58	−12	49
		−6	53	15	52	16	59	18	53	14	51	−10	53	−30	27
		−14	51	11	52	16	65	18	41	15	46	7	47	−4	54
		−18	39	9	64	20	60	15	51	17	49	11	56	6	58
		−22	36	8	67	25	48	19	47	17	51	9	50	−12	48
Average		−14.9†	38.0	11.8	59.8	15.3	55.8	17.5	54.7	16.2	50.1	5.7	53.7	−11.7	43.4
3,280	8.7	−6	50	4	6?	6	46	11	6?	8	50	6	41	−19	41
		−18	41	6	4C	3	68	13	49	15	24	6	38	0	47
		−2	48	7	60	2	47	3	62	5	63	4	55	−21	45
		−12	52	6	61	17	47	18	31	8	47	0	43	−5	55
		−16	52	8	50	10	53	10	53	11	42	3	47	−19	3
		−11	37	13	58	13	48	9	55	5	44	5	58	6	51
		0	57	9	44	15	55	7	46	8	60	0	56	4	49
		6	60	9	36	3	67	12	54	4	?3	9	50	0	44
		5	49	11	53	13	48	12	53	3	40	−2	51	−2	40
		−23	37	7	53	6	61	19	46	1	48	9	52	−8	28
Average		−7.7	48.3	8.0	51.6	8.8	54.0	11.4	51.3	6.8	46.1	4.0	49.1	−6.4	40.3
5,220	5.4	22	21	−4	53	12	38	17	46	9	53	−6	55	−12	42
		5	46	*	4?	19	37	24	36	14	58	5	51	−16	35
		12	4?	,	1?	12	2?	−1?	33	9	53	2	49	−19	17
		1	47	15	37	11	42	20	29	7	46	2	45	−40	17
		18	39	5	45	14	34	16	30	11	3?	?	4?	1?	??
		9	44	7	31	15	31	20	38	10	46	−3	41	−11	3?
		8	25	16	32	20	34	14	40	2	54	5	49	−29	23
		13	26	3	50	15	39	10	52	9	52	5	49	−30	11
		12	37	13	25	15	?1	−26	57	−22	56	0	48	−12	27
		2	38	9	55	6	45	20	47	110	55	0	56	−30	19
Average		10.?	36.9	7.9	41.4	13.9	37.4	12.6	40.8	7.9	50.6	1.6	48.9	−21.3	24.4

* Experimental error, reading not taken.
† Average on the basis of nine readings.
‡ Malfunction of meter reading considered incorrect.
§ Minus readings indicate the height of the pin above the fuze.

TABLE F.2 CHANGE FROM A STATIC TO A DYNAMIC PULSE

Range	UTM Reading	Gap	Range	UTM Reading	Gap	Range	UTM Reading	Gap
feet	mils	mils	feet	mils	mils	feet	mils	mils
3,000	21	55	3,040	25	42	3,080	15	54
	16	60		9	59		13	58
	13	54		15	45		14	44
	8	54		3	73		22	60
	10	44		21	53		16	61
Average	13.2	54.2		15.2	54.6		16.0	59.4
3,120	33	37	3,160	15	59	3,200	17	56
	24	41		17	60		11	45
		48		7	62		9	43
	14	42		13	54		33	46
	13	59		17	37		13	51
Average	18.8	49.4		13.8	54.4		16.4	46.2
3,220	10	55	3,280	14	54	3,400	15	69
	13	59		23	57		6	56
	13	56		9	46		15	63
	16	52		9	54		24	47
	12	44		15	62		23	54
Average	12.8	53.2		14.0	55.0		16.4	56.2
3,440	13	53	3,480	14	56	3,520	10	65
	18	77		12	51		12	62
	14	60		14	47		9	61
	12	68		9	62		18	61
	14	51		20	52		16	51
Average	14.2	61.8		13.6	53.6		13.4	60.0
3,560	11	56	3,600	23	53	3,640	18	54
	22	58		10	56		21	43
	16	46		9	47		15	60
	12	62		21	52		7	66
	15	60		16	52		16	58
Average	15.2	57.6		15.8	56.4		15.4	56.0
3,680	18	61	3,720	13	44	3,760	13	46
	11	51		25	40		21	60
	15	45		23	43		7	44
	17	44		15	42		14	36
	8	66		16	36		19	41
Average	13.8	61.4		18.2	44.8		14.8	57.4
3,800	18	38	3,840	21	59	3,880	15	46
	9	68		11	76		13	45
	20	53		10	56		27	47
	22	45		12	49		13	59
	16	59		18	58		15	41
Average	17.8	52.6		16.8	59.6		16.8	51.6
3,920	13	55	3,960	14	62	4,000	17	56
	13	50		16	57		18	56
	20	51		8	68		16	70
	12	52		11	63		15	40
	8	57		23	36		11	46
Average	13.2	53.6		14.6	57.2		15.4	53.6
4,040	30	36	4,062	30	51	4,120	38	50
	32	45		33	44		21	57
	28	63		31	59		16	46
	8	8		22	62		29	65
	20	33		25	49		27	45
Average	27.5?	44.2?		28.2	55.0		26.6	54.6
4,160	30	69	4,200	25	60	4,240	22	43
	34	53		27	48		21	61
	17	41		20	53		13	71
	19	59		35	56		18	43
	28	50		22	53		19	50
Average	25.?	54.4		25.8	54.0		18.4	53.6

108

SECRET

Range	UTM Reading	Gap	Range	UTM Reading	Gap	Range	UTM Reading	Gap
feet	mils	mils	feet	mils	mils	feet	mils	mils
4,280	32	57	4,320	24	48	4,360	24	49
	27	62		25	59		30	63
	30	51		37	53		21	56
	20	48		17	56		25	54
	18	46		18	59		23	56
Average	23.4	53.2		24.2	59.0		24.4	55.4
4,400	30	56	4,440	24	53	4,400	23	53
	15	57		34	40		31	35
	30	61		25	65		32	60
	24	46		30	63		36	53
	25	46		28	39		25	36
Average	30.8	53.0		36.2	61.8		27.8	49.8
4,520	25	43	4,560	21	56	4,600	21	53
	•	•		19	44		19	52
	21	51		28	44		25	52
	20	48		22	50		20	54
	23	58		27	46		29	46
Average	22.2 †	50.5 †		23.4	48.4		23.4	52.0
4,640	15	56	4,680	20	56	4,720	14	55
	19	61		16	57		15	55
	7	64		20	55		14	45
	19	57		20	50		24	56
	17	50		2	54		7	54
Average	15.4	57.6		15.8	54.4		14.8	53.2
4,760	21	49	4,800	20	49	4,840	18	56
	22	54		24	65		16	36
	21	45		23	57		17	57
	34	37		18	47		18	57
	22	50		16	41		27	37
Average	22.0	45.2		20.0	46.0		19.2	49.8
4,890	12	58	4,920	19	61	4,960	17	48
	8	58		19	62		11	60
	15	51		20	57		14	44
	16	48		16	53		11	53
	14	60		18	55		10	46
Average	12.8	54.6		18.2	55.6		12.6	50.2
5,000	11	69	5,040	19	46	5,080	15	65
	30	54		13	57		6	66
	18	59		17	57		4	61
	10	57		21	55		11	50
	16	37		22	60		6	58
Average	14.0	57.2		18.2	57.0		8.6	59.8
5,120	30	46	5,160	19	61	5,200	14	54
	18	54		12	50		13	56
	24	53		9	51		8	53
	••	61		13	62		12	56
	1	66		24	43		8	58
Average	16.0	56.2		15.4	53.4		11.0	55.4
5,240	9	61	5,280	13	40			
	9	66		8	46			
	•	61		15	47			
	15	56		11	62			
	16	59		14	58			
Average	11.2	60.6		12.2	54.6			

* Gun inoperative - results discarded.
† Average on basis of four.

109

REFERENCES

1. R.D. Thurston and T. Bardeen; "Minefield Clearance"; Project 3.5 , Operation Buster, WT-313, March 1952; Engineer Research and Development Laboratories, Fort Belvoir, Virginia; Unclassified.

2. Owen Richmond; "Minefield Clearance"; Project 3.4, Operation Snapper, WT-526, February 1953; Engineer Research and Development Laboratories, Fort Belvoir, Virginia; Confidential.

3. Owen Richmond; "Minefield Clearance"; Project 3.18, Operation Upshot-Knothole, WT-730, February 1954; Engineer Research and Development Laboratories, Fort Belvoir, Virginia; Confidential Formerly Restricted Data.

4. F. Fleming; "Actuation of Land Mines Under Low Intensity Long Duration Pressure Blast Loading Conditions"; Final Report No. 1, February 1957; Corps of Engineers; Confidential.

5. T.B. Goode and others; "Soil Survey and Backfill Control in Frenchman Flat"; Project 3.8, Operation Plumbbob, ITR-1427, November 1957; U.S. Army Engineer Waterways Experiment Station, Corps of Engineers, Vicksburg, Mississippi; Unclassified.

6. "Capabilities of Atomic Weapons"; TM 23-200, November 1957; Armed Forces Special Weapons Project, Washington, D.C.; Confidential.

7. E.J. Bryant and others; "Basic Air-Blast Phenomena, Part I"; Project 1.1, Operation Plumbbob, ITR-1401, October 1957; Explosion Kinetics Branch, Terminal Ballistics Laboratory, Ballistics Research Laboratories, Aberdeen Proving Ground, Maryland; Confidential Formerly Restricted Data.

8. E.J. Bryant and J.H. Keefer; "Basic Air-Blast Phenomena, Part II"; Project 1.1, Operation Plumbbob, ITR-1481, December 1957; Explosion Kinetics Branch, Terminal Ballistics Laboratory, Ballistics Research Laboratories, Aberdeen Proving Ground, Maryland; Confidential Formerly Restricted Data.

ARMY ACTIVITIES

1   Deputy Chief of Staff for Military Operations, D/A, Washington 25, D.C. ATTN: Dir. of SWAR
2   Chief of Research and Development, D/A, Washington 25, D.C. ATTN: Atomic Div.
3   Assistant Chief of Staff, Intelligence, D/A, Washington 25, D.C.
4- 5   Chief Chemical Officer, D/A, Washington 25, D.C.
6- 7   Chief of Engineers, D/A, Washington 25, D.C. ATTN: ENGNB
8   Chief of Engineers, D/A, Washington 25, D.C. ATTN: ENGEB
9   Chief of Engineers, D/A, Washington 25, D.C. ATTN: ENG-.
10- 11   Office, Chief of Ordnance, D/A, Washington 25, D.C. ATTN: ORDTN
12   Chief Signal Officer, D/A, Plans, Programs, and Ops. Div., Washington 25, D.C. ATTN: SIGOP-7A
13   Chief of Transportation, D/A, Office of Planning and Int., Washington 25, D.C.
14   The Surgeon General, D/A, Washington 25, D.C. ATTN: NEDNE
15- 17   Commanding General, U.S. Continental Army Command, Ft. Monroe, Va.
18   Director of Special Weapons Development Office, Headquarters CONARC, Ft. Bliss, Tex. ATTN: Capt. Chester I. Peterson
19   President, U.S. Army Artillery Board, Ft. Sill, Okla.
20   President, U.S. Army Infantry Board, Ft. Benning, Ga.
21   President, U.S. Army Air Defense Board, Ft. Bliss, Tex. President, U.S. Army Aviation Board, Ft. Rucker, Ala. ATTN: ATBG-DG
22   Commandant, U.S. Army Command & General Staff College, Ft. Leavenworth, Kansas. ATTN: ARCHIVES
23   Commandant, U.S. Army Air Defense School, Ft. Bliss, Tex. ATTN: Command & Staff Dept.
24   Commandant, U.S. Army Armored School, Ft. Knox, Ky.
25   Commandant, U.S. Army Artillery and Missile School, Ft. Sill, Okla. ATTN: Combat Development Department
26   Commandant, U.S. Army Aviation School, Ft. Rucker, Ala.
27   Commandant, U.S. Army Infantry School, Ft. Benning, Ga. ATTN: C.D.S.
28   The Superintendent, U.S. Military Academy, West Point, N.Y. ATTN: Prof. of Ordnance
29   Commandant, The Quartermaster School, U.S. Army, Ft. Lee, Va. ATTN: Chief, QM Library
30   Commandant, U.S. Army Ordnance School, Aberdeen Proving Ground, Md.
31   Commandant, U.S. Army Ordnance and Guided Missile School, Redstone Arsenal, Ala.
32   Commanding General, Chemical Corps Training Comd., Ft. McClellan, Ala.
33   Commandant, USA Signal School, Ft. Monmouth, N.J.
34   Commandant, USA Transport School, Ft. Eustis, Va. ATTN: Security and Info. Off.
35   Commanding General, The Engineer Center, Ft. Belvoir, Va. ATTN: Asst. Cmdt, Engr. School
36   Commanding General, Army Medical Service School, Brooke Army Medical Center, Ft. Sam Houston, Tex.
37   Director, Armed Forces Institute of Pathology, Walter Reed Army Med. Center, 625 16th St., NW, Washington 25, D.C.
38   Commanding Officer, Army Medical Research Lab., Ft. Knox, Ky.
39   Commandant, Walter Reed Army Inst. of Res., Walter Reed Army Medical Center, Washington 25, D.C.
40- 41   Commanding General, QM R&D Comd., QM R&D Cntr., Natick, Mass. ATTN: CBR Liaison Officer

42   Commanding General, Qm. Research and Engr. Comd., USA, Natick, Mass.
43- 44   Commanding General, U.S. Army Chemical Corps, Research and Development Comd., Washington 25, D.C.
45- 46   Commanding Officer, Chemical Warfare Lab., Army Chemical Center, Md. ATTN: Tech. Library
47   Commanding General, Engineer Research and Dev. Lab., Ft. Belvoir, Va. ATTN: Chief, Tech. Support Branch
48   Director, Waterways Experiment Station, P.O. Box 631, Vicksburg, Miss. ATTN: Library
49   Commanding Officer, Office of Ordnance Research, Box CM, Duke Station, Durham, North Carolina
50   Commanding Officer, Picatinny Arsenal, Dover, N.J. ATTN: ORDBB-TK
51   Commanding Officer, Diamond Ord. Fuze Labs., Washington 25, D.C. ATTN: Chief, Nuclear Vulnerability Br. (230)
52- 53   Commanding General, Aberdeen Proving Grounds, Md. ATTN: Director, Ballistics Research Laboratory
54   Commanding General, Frankford Arsenal, Bridge and Tacony St., Philadelphia, Pa.
55   Commanding Officer, Watervliet Arsenal, Watervliet, New York. ATTN: ORDBF-RR
56- 57   Commanding General, U.S. Army Ord. Missile Command, Redstone Arsenal, Ala.
58   Commanding General, Ordnance Tank Automotive Command, Detroit Arsenal, Centerline, Mich. ATTN: CRDMC-RO
59   Commanding General, Ordnance Ammunition Command, Joliet, Ill.
60   Commanding General, Ordnance Weapons Command, Rock Island, Ill.
61   Commanding Officer, USA Signal R&D Laboratory, Ft. Monmouth, N.J.
62   Commanding General, U.S. Army Electronic Proving Ground, Ft. Huachuca, Ariz. ATTN: Tech. Library
63   Commanding Officer, USA, Signal R&D Laboratory, Ft. Monmouth, N.J. ATTN: Tech. Doc. Ctr., Evans Area
64   Commanding Officer, USA Transportation Research Command, Ft. Eustis, Va. ATTN: Chief, Tech Info. Div.
65   Commanding Officer, USA Transportation Combat Development Group, Ft. Eustis, Va.
66   Director, Operations Research Office, Johns Hopkins University, 6935 Arlington Rd., Bethesda 14, Md.
67   Commanding General, U. S. ORD Special Weapons-Ammunition Command, Dover, N.J.
68   Commander-in-Chief, U.S. Army Europe, APO 403, New York, N.Y. ATTN: Opot. Div., Weapons Br.
69   Commanding Officer, 9th Hospital Center, APO 180, New York, N.Y. ATTN: CO, US Army Nuclear Medicine Research Detachment, Europe

NAVY ACTIVITIES

70   Chief of Naval Operations, D/N, Washington 25, D.C. ATTN: OP-03EG
71   Chief of Naval Operations, D/N, Washington 25, D.C. ATTN: OP-31
72   Chief of Naval Operations, D/N, Washington 25, D.C. ATTN: OP-75
73   Chief of Naval Operations, D/N, Washington 25, D.C. ATTN: OP-91
74   Chief of Naval Operations, D/N, Washington 25, D.C. ATTN: OP-92201
75- 76   Chief of Naval Research, D/N, Washington 25, D.C. ATTN: Code 811

77-79 Chief, Bureau of Naval Weapons, D/N, Washington 25, D.C. ATTN: DLI-3

80 Chief, Bureau of Medicine and Surgery, D/N, Washington 25, D.C. ATTN: Special Wpns. Def. Div.

81 Chief, Bureau of Ordnance, D/N, Washington 25, D.C.

82 Chief, Bureau of Ships, D/N, Washington 25, D.C. ATTN: Code 423

83 Chief, Bureau of Yards and Docks, D/N, Washington 25, D.C. ATTN: D-440

84 Director, U.S. Naval Research Laboratory, Washington 25, D.C. ATTN: Mrs. Katherine H. Cass

85-86 Commander, U.S. Naval Ordnance Laboratory, White Oak, Silver Spring 19, Md.

87 Commanding Officer and Director, Navy Electronics Laboratory, San Diego 52, Calif.

88 Commanding Officer, U.S. Naval Mine Defense Lab., Panama City, Fla.

89-90 Commanding Officer, U.S. Naval Radiological Defense Laboratory, San Francisco, Calif. ATTN: Tech. Info. Div.

91-92 Commanding Officer and Director, U.S. Naval Civil Engineering Laboratory, Port Hueneme, Calif. ATTN: Code L31

93 Commanding Officer, U.S. Naval Schools Command, U.S. Naval Station, Treasure Island, San Francisco, Calif.

94 Superintendent, U.S. Naval Postgraduate School, Monterey, Calif.

95 Commanding Officer, Nuclear Weapons Training Center, Atlantic, U.S. Naval Base, Norfolk 11, Va. ATTN: Nuclear Warfare Dept.

96 Commanding Officer, Nuclear Weapons Training Center, Pacific, Naval Station, San Diego, Calif.

97 Commanding Officer, U.S. Naval Damage Control Tng. Center, Naval Base, Philadelphia 12, Pa. ATTN: ABC Defense Course

98 Commanding Officer, Air Development Squadron 5, VX-5, China Lake, Calif.

99 Commanding Officer, Naval Air Material Center, Philadelphia 12, Pa. ATTN: Technical Data Br.

100 Commander, Officer U.S. Naval Air Development Center, Johnsville, Pa. ATTN: NAS, Librarian

101 Commanding Officer, U.S. Naval Medical Research Institute, National Naval Medical Center, Bethesda, Md.

102 Commanding Officer and Director, David W. Taylor Model Basin, Washington 7, D.C. ATTN: Library

103 Officer-in-Charge, U.S. Naval Supply Research and Development Facility, Naval Supply Center, Bayonne, N.J.

104 Commandant, U.S. Marine Corps, Washington 25, D.C. ATTN: Code AO3H

105 Director, Marine Corps Landing Force, Development Center, MCS, Quantico, Va.

106 Commanding Officer, U.S. Naval CIC School, U.S. Naval Air Station, Glynco, Brunswick, Ga.

107-108 Chief, Bureau of Naval Weapons, Navy Department, Washington 25, D.C. ATTN: RRU2

AIR FORCE ACTIVITIES

109 Hq. USAF, ATTN: Operations Analysis Office, Office, Vice Chief of Staff, Washington 25, D.C.

110 Director of Civil Engineering, Hq. USAF, Washington 25, D.C. ATTN: AFOCE

111-112 Air Force Intelligence Center, Hq. USAF, ACS/I (AFCIN-3V1) Washington 25, D.C.

113 Director of Research and Development, DCS/D, Hq. USAF, Washington 25, D.C. ATTN: Guidance and Weapons Div.

114 The Surgeon General, Hq. USAF, Washington 25, D.C. ATTN: Bio.-Def. Pre. Med. Division

115 Commander, Tactical Air Command, Langley AFB, Va. ATTN: Doc. Security Branch

116 Commander, Air Defense Command, Ent AFB, Colorado. ATTN: Assistant for Atomic Energy, ADLDC-A

117 Commander, Hq. Air Research and Development Command, Andrews AFB, Washington 25, D.C. ATTN: RDRWA

118 Commander, Air Force Ballistic Missile Div., HQ ARDC, Air Force Unit Post Office, Los Angeles 45, Calif. ATTN: WDSOT

119-120 Commander, AF Cambridge Research Center, L.G. Hanscom Field, Bedford, Mass. ATTN: CRQST-2

121-125 Commander, Air Force Special Weapons Center, Kirtland AFB, Albuquerque, N. Mex. ATTN: Info. & Intel.

126-127 Director, Air University Library, Maxwell AFB, Ala.

128 Commander, Lowry Technical Training Center (TW), Lowry AFB, Denver, Colorado.

129 Commandant, School of Aviation Medicine, Brooks Air Force Base, Texas.

130 Commander, 1009th Sp. Wpns. Squadron, Hq USAF, Washington 25, D.C.

131-133 Commander, Wright Air Development Center, Wright-Patterson AFB, Dayton, Ohio. ATTN: WCOSI (2)

134-135 Director, USAF Project RAND, VIA: USAF Liaison Office, The RAND Corp., 1700 Main St., Santa Monica, Calif.

136 Commander, Rome Air Development Center, ARDC, Griffiss AFB, N.Y. ATTN: Documents Library, RCSSL

137 Commander, Air Technical Intelligence Center, USAF, Wright-Patterson AFB, Ohio. ATTN: ACIN-4E1a

138 Assistant Chief of Staff, Intelligence, Hq. USAFE, APO 633, New York, N.Y. ATTN: Directorate of Air Targets

139 Commander-in-Chief, Pacific Air Forces, APO 953, San Francisco, Calif. ATTN: PFCIE-MB, Base Recovery

OTHER DEPARTMENT OF DEFENSE ACTIVITIES

140 Director of Defense Research and Engineering, Washington 25, D.C. ATTN: Tech. Library

141 Chairman, Armed Services Explosives Safety Board, DOD, Building T-7, Gravelly Point, Washington 25, D.C.

142 Director, Weapons Systems Evaluation Group, Room 1E880, The Pentagon, Washington 25, D.C.

143-146 Chief, Defense Atomic Support Agency, Washington 25, D.C. ATTN: Document Library

147 Commander, Field Command, DASA, Sandia Base, Albuquerque, N. Mex.

148-149 Commander, Field Command, DASA, Sandia Base, Albuquerque, N. Mex. ATTN: FCTG

150-154 Commander, Field Command, DASA, Sandia Base, Albuquerque, N. Mex. ATTN: FCWT

155 Commander-in-Chief, Strategic Air Command, Offutt AFB, Neb. ATTN: OAWS

156 U.S. Documents Officer, Office of the United States National Military Representative - SHAPE, APO 55, New York, N.Y.

ATOMIC ENERGY COMMISSION ACTIVITIES

157-159 U.S. Atomic Energy Commission, Technical Library, Washington 25, D.C. ATTN: For DMA

160-161 Los Alamos Scientific Laboratory, Report Library, Box 1663, Los Alamos, N. Mex. ATTN: Helen Redman

162-166 Sandia Corporation, Classified Document Division, Sandia Base, Albuquerque, N. Mex. ATTN: J. D. Smyth, Jr.

167-176 University of California Lawrence Radiation Laboratory, P.O. Box 808, Livermore, Calif. ATTN: Clovis G. Craig

177 Weapon Data Section, Technical Information Service Extension, Oak Ridge, Tenn.

178-210 Technical Information Service Extension, Oak Ridge, Tenn. (Surplus)

119